Cellular and Molecular Life Sciences (2024) 81:422
https://doi.org/10.1007/s00018-024-05452-4

ORIGINAL ARTICLE

SENP1 mediates zinc-induced ZnT6 deSUMOylation at Lys-409 involved in the regulation of zinc metabolism in Golgi apparatus

Chang-Chun Song[1] · Tao Liu[1] · Christer Hogstrand[4] · Chong-Chao Zhong[1] · Hua Zheng[1] · Lv-Hui Sun[3] · Zhi Luo[1,2]

Received: 1 July 2024 / Revised: 10 September 2024 / Accepted: 16 September 2024

Abstract

Zinc (Zn) transporters contribute to the maintenance of intracellular Zn homeostasis in vertebrate, whose activity and function are modulated by post-translational modification. However, the function of small ubiquitin-like modifier (SUMOylation) in Zn metabolism remains elusive. Here, compared with low Zn group, a high-Zn diet significantly increases hepatic Zn content and upregulates the expression of metal-response element-binding transcription factor-1 (MTF-1), Zn transporter 6 (ZnT6) and deSUMOylation enzymes (SENP1, SENP2, and SENP6), but inhibits the expression of SUMO proteins and the E1, E2, and E3 enzymes. Mechanistically, Zn triggers the activation of the MTF-1/SENP1 pathway, resulting in the reduction of ZnT6 SUMOylation at Lys 409 by small ubiquitin-like modifier 1 (SUMO1), and promoting the deSUMOylation process mediated by SENP1. SUMOylation modification of ZnT6 has no influence on its localization but reduces its protein stability. Importantly, deSUMOylation of ZnT6 is crucial for controlling Zn export from the cytosols into the Golgi apparatus. In conclusion, for the first time, we elucidate a novel mechanism by which SUMO1-catalyzed SUMOylation and SENP1-mediated deSUMOylation of ZnT6 orchestrate the regulation of Zn metabolism within the Golgi apparatus.

Keywords Zinc · Zinc transporter · MTF-1 · SUMOylation · SENP1 · Zn homeostasis

Abbreviations

B2M	Beta-2 microglobulin
CHX	Cycloheximide
Cu	Copper
DMEM	Dulbecco's Modified Eagles Medium
ELFA	Translation elongation factor
EMSA	Electrophoretic mobility-shift assay
FBS	Fetal bovine serum
GAPDH	Glyceraldehyde-3-phosphate dehydrogenase
HEK-293T	Human embryonic kidney 293T cell
HPRT	Hypoxanthine-guanine phosphoribosyl transferase
ICP-OES	Inductively coupled plasma optical emission spectrometry
Fe	Iron
Mn	Manganese
MRE	Metal responsive element
MTF-1	Metal-responsive transcription factor-1
NEM	N-ethylmaleimide
PIAS1	Protein inhibitor of activated STAT 1
qRT-PCR	Real-time quantitative PCR
RPL7	Ribosomal protein L7
SAE1	SUMO1-activating enzyme subunit 1
SEM	Standard error of means
SENP	SUMO-specific peptidase
SUMO1/2/3	Small ubiquitin related modifiers 1/2/3
TPEN	N, N,N′,N′- tetrakis (2-pyridylmethyl)-ethylenediamine

✉ Zhi Luo
luozhi99@mail.hzau.edu.cn; luozhi99@aliyun.com

[1] Hubei Hongshan Laboratory, Fishery College, Huazhong Agriculture University, Wuhan 430070, China

[2] Laboratory for Marine Fisheries Science and Food Production Processes, Qingdao National Laboratory for Marine Science and Technology, Qingdao 266237, China

[3] State Key Laboratory of Agricultural Microbiology, Hubei Hongshan Laboratory, Frontiers Science Center for Animal Breeding and Sustainable Production, College of Animal Sciences and Technology, Huazhong Agricultural University, Wuhan 430070, China

[4] Diabetes and Nutritional Sciences Division, School of Medicine, King's College London, London, UK

Published online: 05 October 2024

UBC9	SUMO-conjugating enzyme
UBCE	Ubiquitin-conjugating enzyme
Zn	Zinc
ZnT6	Zinc transporter 6

Introduction

Zinc (Zn) is an important micro-mineral essential for many physiological processes in vertebrates, including DNA transcription, growth and nutrient metabolism [1–3]. However, excess Zn accumulation is cytotoxic, associated with oxidative stress, dysregulation of glucose and lipid metabolism, impaired immune function and cardiovascular disease [3–6]. Consequently, maintaining an adequate intracellular Zn level is crucial to prevent the potential toxicity of excessive Zn accumulation.

The regulation of cellular Zn homeostasis is tightly controlled by two Zn transporter families (the SLC30A/ZnTs family and SLC39A/ZIPs family), coupled with storage proteins metallothioneins (MTs). ZnTs family members, including ZnT1–10, are responsible for reducing cytosolic Zn contents by facilitating Zn export from the cytosols into the intracellular compartmentalization or out of the cells [7, 8]. Metal-responsive transcription factor 1 (MTF-1) functions as the only cellular Zn-sensing transcription factor in vertebrates, playing a critical role in governing intracellular Zn levels by binding to the metal response element (MRE) and transcriptionally activating its target genes in response to elevated cytosolic Zn^{2+} concentrations [9]. However, much remains to be understood in terms of control of zinc trafficking within cells and its significance in terms of cell function.

As a membrane organelle, the Golgi apparatus exists in most eukaryotic cells and plays a variety of functions, including membrane trafficking, posttranslational modification and protein sorting [10]. Metal ions in the Golgi lumen are essential for the maintaining the proper structure and functions of Golgi apparatus [11]. Among these, Zn functions as an indispensable cofactor for many secretory enzymes, participating in the substrate specificity and catalytic activity of the enzyme [12]. However, abnormal Zn accumulation in the Golgi apparatus impairs its function. Therefore, the Golgi Zn homeostasis needs to be tightly regulated by corresponding transporters. ZnT6, as a member of ZnT family, localizes to Golgi apparatus and plays pivotal roles in transporting Zn from cytoplasm to Golgi apparatus [7, 13]. However, mammalian ZnT6 orthologs don't have transporter activity by themselves but depend on heterodimerisation to other ZnT family proteins for function [14, 15]. Recent studies indicated that ZnT5 recruits ZnT6 to the Golgi apparatus to form the functional ZnT5–ZnT6 heterodimers that are required for activating zinc ectoenzymes [16]. However, it remains unknown whether ZnT6 also need to form heterodimers to be activated in other species except mammals. Thus, investigating the subcellular localization, function and regulatory mechanism of ZnT6 are significant, which helps to elucidate the mechanism of Zn homeostasis in Golgi apparatus and provide potential targets for protection against the diseases induced by Zn disorders.

SUMOylation is an important post-translational modification that covalently conjugates small ubiquitin related modifiers (SUMO) to Lys residues of the target protein. SUMOylation modification of the protein plays an essential role in protein activity, sub-cellular localization, stabilization and protein-protein interactions [17–19]. Three SUMO isoforms (SUMO1, SUMO2, and SUMO3) have been identified in mammals [20]. SUMOylation modification is catalyzed by specific enzymes, including activating enzyme E1 (SAE1/UBA2), conjugating enzyme E2 (UBC9), and ligating enzyme E3 ligase, which can be reversed by SUMO-specific proteases (SENPs) [19, 21]. In mammals, six SENPs (SENP1-3 and SENP5-7) have been reported to be involved in the deSUMOylation process, which have different preference for SUMO proteins [22]. Furthermore, SUMOylation regulates multiple biological processes, and also plays important roles in the tissue homeostasis [21]. At present, few reports have investigated the link between SUMOylation modification and the control of Zn homeostasis. To our best knowledge, only one study has reported that SUMOylation is involved the regulation of Zn sensor MTF-1 [23]. Recently, Thingholm et al. [24] published an influential review in *Cell Mol Life Sci*, which summarized the function and regulatory mechanism of Zn transporters and focused on the effect of phosphorylation modification on the function of Zn transporters. However, the research on SUMO modification of zinc transporters remains largely unexplored. Therefore, further exploration is required to elucidate the regulatory mechanism of SUMOylation modification in regulating Zn metabolism.

Among the vertebrates, fish comprise approximately half of all vertebrate species (about 30,000 species reported) and represent the most diverse and widely distributed vertebrate group worldwide [25, 26]. Despite evolutionary distinction between fish and mammals, their metabolic processes display striking conservation [27]. Consequently, fish provide good models for investigating the functions and regulation of genes, and in turn the metabolism and physiology. Given that Zn is an indispensable trace element in fish, dietary Zn deficiency and excess may disturb cellular Zn distribution, and are associated with various disorders, including growth retardation, immune dysfunction, fatty liver and tissues damage [28–30]. Thus, the Zn homeostasis needs to be

controlled within an appropriate range with the assistance of Zn transporters. Our previous studies have elucidated the regulatory mechanisms of several Zn transporters in response to Zn at transcription and translation levels, using yellow catfish *Pelteobagrus fulvidraco*, an ecologically and economically freshwater fish in Asian countries, as the model [31, 32]. Nevertheless, the complexities of Zn regulation in cells remain largely unexplored. Although the phosphorylation of ZIP7 by CK2 leading to ZIP7-mediated zinc release from the ER has been investigated [33], currently the mechanism SUMOylation modification of Zn transporters is still unclear. As a continuation of our study involved in their function and the regulatory mechanism of Zn transporters, the present study investigates whether and how the SUMOylation of Zn transporters mediates Zn metabolism. Here we reveal that SUMOylation modification is a previously unexplored mechanism to regulate zinc transporters and that SUMOylation modification of ZnT6 controls Zn uptake into the Golgi apparatus.

Experimental procedures

Ethical statement

All studies protocols involving animal experimentation were conducted with the guidance and approval of Huazhong Agricultural University Animal Ethics Committees.

Animals feeding, management and sampling

The protocols of the feeding trials in yellow catfish were similar to our recent studies [34]. Three experimental diets were produced with $ZnSO_4 \cdot 7H_2O$ supplemented at levels of 0 (low Zn, L-Zn, without extra Zn addition), 0.03 (middle Zn, M-Zn,) and 0.45 (high Zn, H-Zn) g kg^{-1} diet. Final dietary Zn content in the three experimental diets were detected by ICP-OES (Optima 8000DV, PerkinElmer, USA), whose content were 12.10, 18.69 and 120.82 mg/kg for the L-Zn, M-Zn and H-Zn groups, respectively. According to previous study [28], the middle dietary Zn (M-Zn) was optimal in meeting dietary Zn requirement for *P. fulvidraco*. The detailed experimental procedures and sampling methods were similar to those in our previous studies [35], and the details are presented in Text S1.

Cell culture and treatments

According to previous study [1], the primary hepatocytes were isolated from the liver of yellow catfish and cultured in M199 medium (#11150099, Thermo Fisher Scientific) media in the presence of 10% fetal bovine serum (FBS) (#10099141, Thermo Fisher Scientific) in a 28℃ incubator. HEK-293T cells were purchased from the Cell Resource Center of HZAU and used for the analysis of protein-protein interaction, SUMOylation sites and promoter function. They were grown in Dulbecco's Modified Eagle's medium (DMEM, #11965092, Thermo Fisher Scientific) media supplemented with 10% fetal bovine serum (FBS) (#10099141, Thermo Fisher Scientific), and cultured at 37 ˚C with 5% CO_2. To determine the mechanistic role of SUMOylation in mediating the alterations of ZnT6 expression induced by Zn, hepatocytes were treated with N, N,N',N'-Tetrakis (2-pyridylmethyl) ethylenediamine (TPEN, Zn chelator, 2 μM, #P4413, Sigma-Aldrich). TPEN was added 2 h prior to Zn addition (70 μM). $2–5 \times 10^6$ cells were used for the following experiments. The concentrations and treatment time of Zn and TPEN were based on our previous publications [1, 3]. For the protein stability assay, cells were treated with cycloheximide (100 μg/ml, Sigma) for different times to inhibit protein synthesis, according to previous study [36]. After 48 h of treatment, the cells were harvested for subsequent analysis.

Cell viability assay

The CCK-8 assay kit (#C0037, Beyotime Biotechnology, Shanghai, China) was used to determine the cell viability according to the manufacture's instruction. The detailed methods were described in Text S2.

Reverse transcription and real-time quantitative PCR (qRT-PCR)

Total RNA was extracted from cultured cells or liver tissue using TRIzol reagent (Thermo Fisher Scientific, Waltham, MA, USA) following the manufacturer's protocol. qPCR assays were performed to quantify the RNA abundance of target genes, as described in our previous protocols [37]. The detailed procedures were shown in Text S3. All date were analyzed by the $2^{-\Delta\Delta Ct}$ method to determine their relative transcript levels. The sequences of PCR primers were listed in Table S1.

Western blot analysis, immunoprecipitation and immunofluorescence staining

Western blotting was quantitatively analyzed by Image-Pro Plus 6.0 software (Media Cybernetics) to detect protein level, following our published protocol [37]. The detailed methods were provided in Text S4.

Immunoprecipitation was performed to investigate the SUMOylation of target protein and protein-protein interactions. Immunofluorescent staining was conducted to detect

the expression, subcellular distribution and interactions of the target proteins, as previously described [3]. The detailed experimental procedures of co-immunoprecipitation and immunofluorescence staining were described in Text S5.

Plasmids construction, short interfering RNAs and transfections

To identify whether ZnT6 can be SUMOylated and what function ZnT6 SUMOylation modification plays, the ZnT6, SUMO1, SUMO2, SUMO3, UBC9 and SENPs (1, 2, 3, 5, 6, 7 and 8) overexpression vectors were generated as described previously [37]. The details procedures were provided in Text S6. The primers sequences for plasmids construction and site mutagenesis were shown in Table S2.

To confirm the roles of MTF-1 and SENP1 in Zn-induced changes of Zn transporter and determine which Zn transporter could be SUMOylated, the experiments were carried out to knock-down the expression of MTF-1 and SENP1. For knockdown experiments, the siRNA sequences targeting SENP1 and MTF-1 were synthesized by Genepharma Biotech company (Shanghai, China) and transiently transfected into cells using the Entranster^{TM}-R4000 Transfection Reagent (Engreen Corp, Beijing, China) according to the manufacturer's instructions. Based on the qPCR and western blot analysis, the siRNA sequence with the highest knockdown efficiency was selected from three pairs of siRNA sequences for the further experimentation. The sequences of siRNAs are shown in Table S3.

Cycloheximide (CHX) assay

To detect the protein stability of ZnT6, HEK-293T cells (2×10^5) were transfected with corresponding overexpression plasmids; primary hepatocytes of yellow catfish were transfected with siRNAs targeting *senp1*. After treatment with CHX (#239763-M, 100 μg/mL, Sigma, St Louis, MO, USA) for the corresponding time, these cells were then collected and lysed by lysis buffer for subsequent western blotting analysis.

Subcellular fractionation and measurement of Zn, Fe, Cu and Mn contents

Extraction of the Golgi apparatus was performed according to the instructions of the Cell/tissue Golgi apparatus extraction Kit (#BB-3604, Bestbio company, Shanghai, China). After the Golgi apparatus were isolated, their protein concentrations were measured using the bicinchoninic acid (BCA) method. Then, according to previous study [38], ICP-OES was used to detect the content of Zn in liver tissue and Golgi apparatus, as well as the contents of Fe, Cu and Mn in cells.

Promoter cloning and dual luciferase reporter assay

The *senp1* promoter was constructed into the pGL3 basic vector based on the available genome sequence of yellow catfish [39]. The MTF-1 binding site (MRE) in the *senp1* promoter was predicted via the JASPAR database. Subsequently, the MRE site was mutated from the pGl3-*senp1*-951/+99 plasmid using the QuickChange II Site-Directed Mutagenesis Kit (Vazyme, NJ, US), following the manufacturer's protocol. The sequences of mutagenesis primers were shown in Table S4. Furthermore, the Dual-Luciferase Reporter Assay System (Promega, Minneapolis, MN, USA) was used to measure the promoter activity of *senp1*.

Electrophoretic mobilityshift assay (EMSA)

Extraction of the nuclear proteins were performed with a commercial kit (#P0027, Beyotime Company, Shanghai, China) from the yellow catfish hepatocytes and HEK-293T cells, and the concentration was measured using the bicinchoninic acid method. Subsequently, to investigate the binding ability of MTF-1 to *senp1* promoter, the EMSA was performed as our published protocol [32]. The experimental procedures of EMSA were shown in Text S7 in detail. The nucleotide sequences of probe and competitors were provided in Table S4.

Statistical analysis

Statistical analysis was performed using SPSS 19.0 software (Armonk, NY, USA). All data values were shown as means ± SEM (standard errors of means) of at least three independent experiments. For three treatments comparisons (low, middle and high Zn), one-way analysis of variance was used with a post hoc Duncan's multiple range test. The Student's *t*-test was conducted for the comparison of the differences between two groups. A P value < 0.05 indicates statistically significant difference.

Results

In vivo studies

Dietary zn addition increased hepatic zn accumulation and induced ZnT6 and MTF-1 expression, and promoted MTF-1 nuclear translocation

To investigate the effects of dietary Zn supplementation on hepatic Zn metabolism, we determined hepatic Zn content, and the expression of genes related to Zn metabolism. Zn content of liver and hepatic Golgi apparatus increased with dietary Zn levels (Fig. 1a and b). Compared with the L- and M-Zn groups, H-Zn up-regulated the *znt6* and *mtf-1* mRNA abundance (Fig. 1c and d), and increased the protein levels of ZnT6, total-MTF-1 and nuclear-MTF-1 (Fig. 1e and f). Moreover, immunofluorescence staining corroborated the Zn-dependent upregulation of ZnT6 and MTF-1 at protein levels (Fig. 1g and h). Overall, these results suggested that high dietary Zn led to hepatic Zn overload, increased ZnT6 and MTF-1 expression, and promoted MTF-1 nuclear translocation.

Dietary zn addition influenced SUMOylation progress in the liver

Since Zn has been found to influence SUMOylation modification [40], we investigated the effects of dietary Zn supplementation on the expression of genes involved in SUMOylation at the protein and mRNA levels. Our results showed that high dietary Zn reduced SUMO1 protein expression but increased the SUMO-specific proteases (SENP1 and SENP2) protein levels. Among three dietary groups, SUMO2/3 protein expression was highest in M-Zn group, and the lowest in H-Zn group. Compared with the L-Zn group, H-Zn diet significantly reduced the protein levels of E1-activating enzyme SAE1, E2-conjugating enzyme UBC9 and E3 ligase PIAS1, respectively (Fig. 2a and b). Immunofluorescence staining corroborated the Zn-dependent reduction of SUMO1 expression and increase of SENP1 expression (Fig. 2c and d).

At the transcriptional level, H-Zn diet down-regulated the *sumo1*, *sae1*, *ubc9* and *pias1* mRNA levels, but up-regulated the *senp2* and *senp6* mRNA expression, compared to the other two groups. Among three dietary groups, *sumo3* mRNA expression was highest, and *senp3* mRNA expression was lowest for fish fed the M-Zn diet. The mRNA expression of *senp1* was significantly lower in L-Zn group than that in other two groups. The *sumo2*, *senp5*, *senp7* and *senp8* mRNA expression was not significantly affected by dietary Zn supplementation (Fig. 2e). Overall, these results indicated that high dietary Zn addition inhibited SUMOylation modification through increasing the expression of SUMO-specific proteases.

In vitro studies

Zn affected Zn metabolism, induced intracellular zn deposition and modulated SUMOylation modification in yellow catfish hepatocytes

To further investigated the effect of Zn incubation on Zn metabolism, as well as the expression of SUMOylation-related genes, hepatocytes were isolated from yellow catfish, and TPEN was used to chelate the Zn. The CCK-8 assay demonstrated that 0–70 μM Zn did not remarkably affect the viability of yellow catfish hepatocytes (Fig. S1A). In order to explore whether the addition of Zn and TPEN affects other transition elements, the contents of Zn, Fe, Cu and Mn in cells were detected. TPEN could not only reduce the intracellular Zn content, but also alleviate the increase of intracellular Zn content induced by excessive Zn addition (Fig. S1B). However, the addition of Zn or TPEN had no significant effect on the contents of other transition elements in the cells, including Fe, Cu and Mn (Fig. S1C-E). Furthermore, TPEN pre-incubation alleviated the Zn-induced increase in ZnT6 protein levels (Fig. 3a and b). Compared with control group, Zn increased *znt6* mRNA expression, while TPEN pretreatment significantly alleviated the changes induced by Zn (Fig. 3c). Considering that ZnT5 can form a heterodimer with ZnT6, we also detected the protein expression of ZnT5. Our result indicated that TPEN treatment alleviated the increase of ZnT5 protein expression induced by Zn addition (Fig. S1F and G). Moreover, TPEN pre-incubation remarkably blunted the Zn-induced accumulation of Zn in the Golgi apparatus (Fig. 3d). Using the Newport green DCF Diacetate (N7991) probe, we found that 70 μM Zn treatment increased intracellular Zn content and its co-localization with the Golgi apparatus, while TPEN pre-treatment abrogated these changes (Fig. 3e). Thus, Zn supplementation promoted the transport of Zn into Golgi apparatus.

Compared with the control, Zn incubation down-regulated the protein levels of SUMO1, SUMO2/3, SAE1, UBC9 and PIAS1, but up-regulated the protein expression of SENP1, and TPEN pretreatment alleviated these changes in protein levels induced by Zn (Fig. 3f and g). Furthermore, pre-incubation with TPEN remarkably inhibited Zn-induced increase in the ZnT6 and SENP1 protein levels, and decreased the co-localization of ZnT6 with SENP1, which indicated that Zn incubation potentially promoted the deSUMOylation of ZnT6 by SENP1 (Fig. 3h). Compared to the control, Zn incubation increased the mRNA levels of *senp1*, *senp2*, *senp6* and *senp8*, and decreased the mRNA

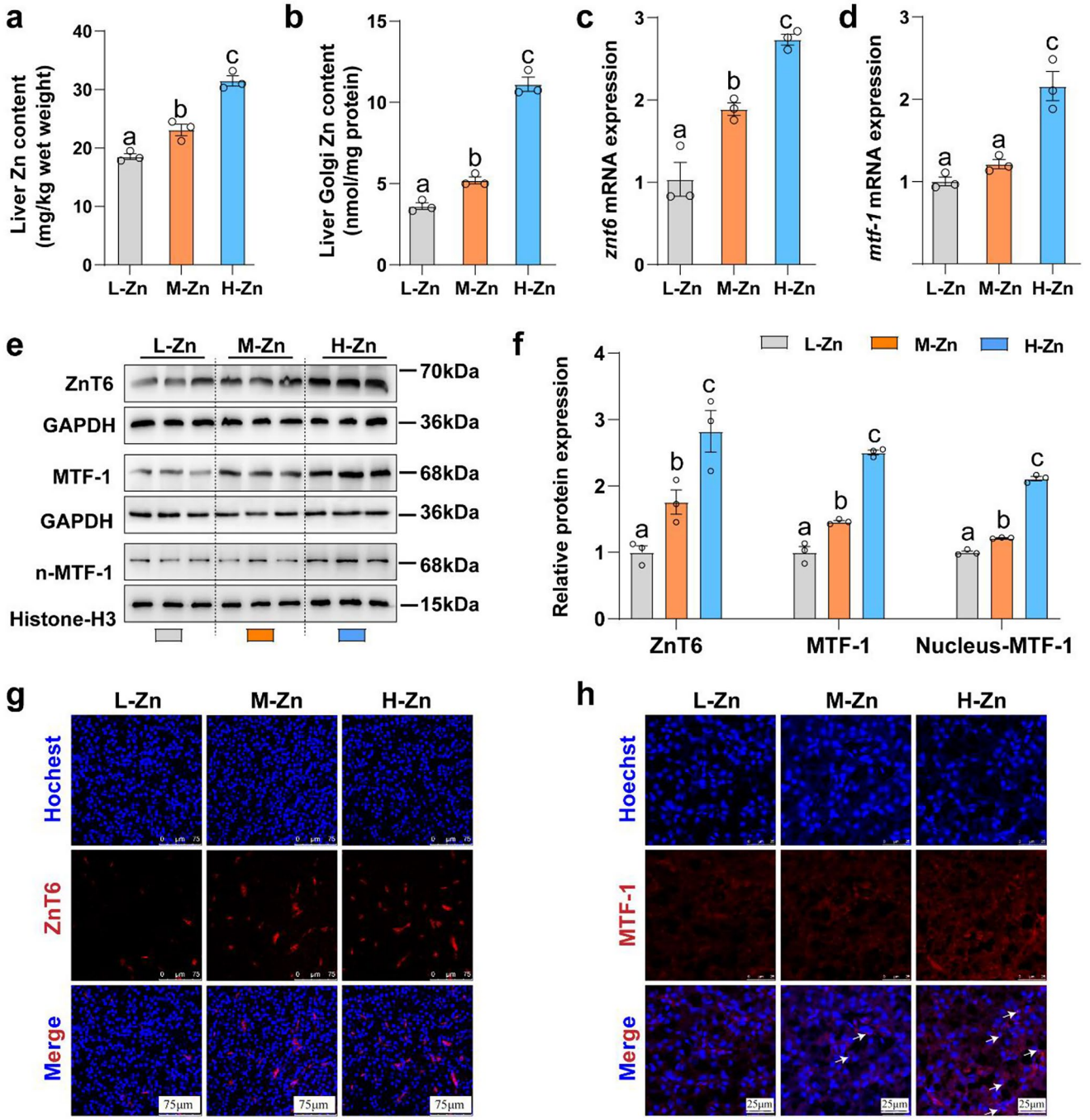

Fig. 1 Effects of dietary Zn levels on Zn metabolism in the liver of yellow catfish. (**a**), Zn content in the liver. (**b**), Zn content in the Golgi apparatus of the liver tissue. (**c**) and (**d**), mRNA levels of *znt6* (**c**) and *mtf-1* (**d**). (**e-f**) Western blot (**e**) and quantification (**f**) analysis of ZnT6, MTF-1 and n-MTF-1 (nucleus-MTF-1). (**g**), Immunofluorescent analysis of ZnT6. Scale bars, 75 μm. (**h**), Immunofluorescent analysis of MTF-1. Scale bars, 25 μm. Values represent the means ± SEM ($n = 3$ replicate tanks, and 6 fish were sampled from each tank). Significant variations at $P < 0.05$ are denoted by the Letter (a-c)

abundance of *sumo1*, *sumo3*, *sae1*, *ubc9* and *pias1*, while these changes were abolished by TPEN pre-incubation (Fig. S1H). Collectively, the above findings suggested that Zn treatment affected the absorption and transport of Zn, led to accumulation of Zn in Golgi apparatus, and modulated SUMOylation modification.

Zn regulated senp1 transcription via MTF-1 binding to its promoter

Considering that high dietary Zn up-regulated the mRNA and protein levels of *mtf-1* and *senp1*, and also promoted translocation of MTF-1 to the nucleus, we conducted in

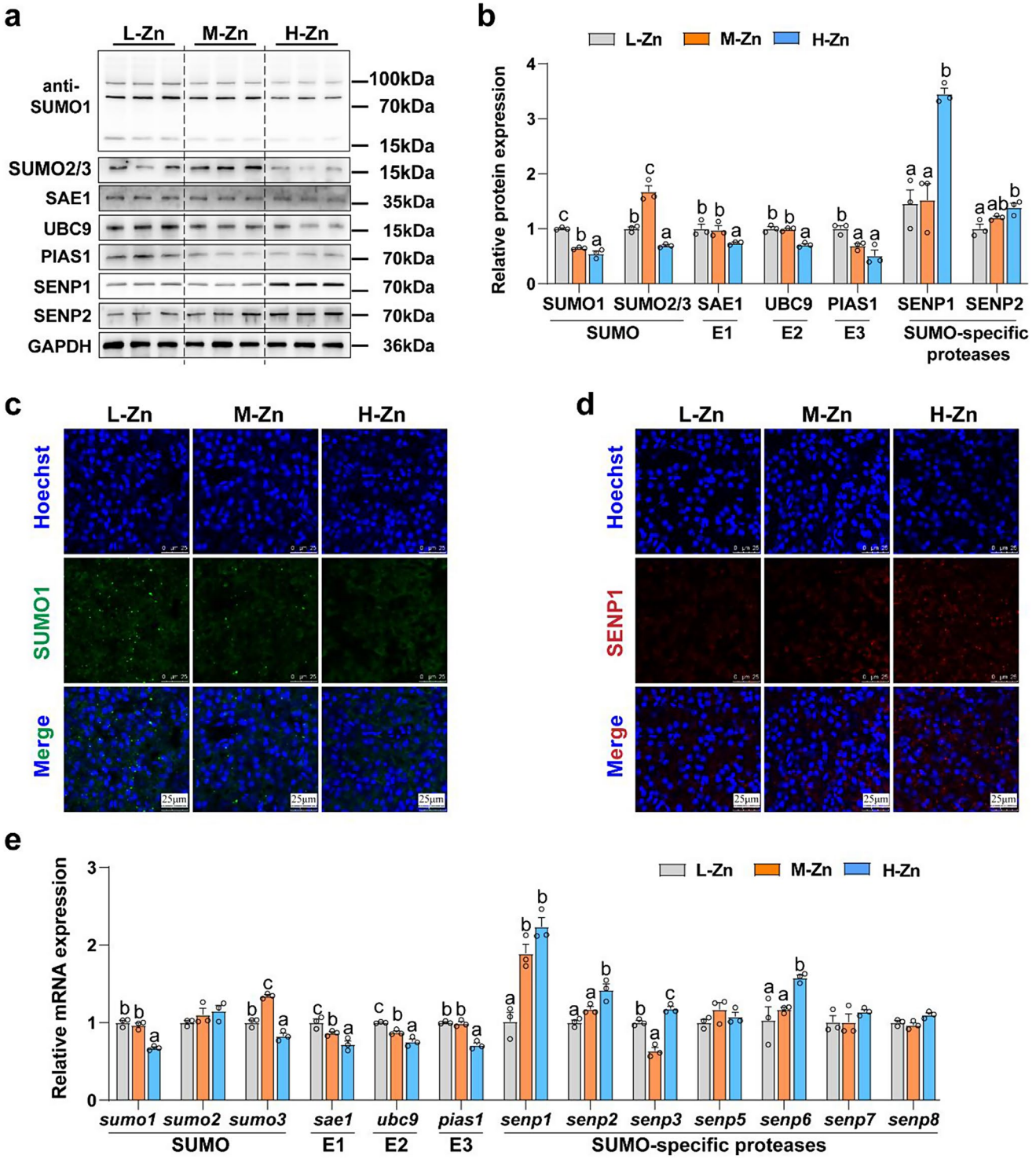

Fig. 2 Effects of dietary Zn levels on SUMOylation progress in the liver of yellow catfish. (**a** and **b**), Western blot (**a**) and statistical analysis (**b**) of the protein involved in pro-SUMOylation (SUMO1, SUMO2/3, SAE1, UBC9 and PIAS1) and de-SUMOylation (SENP1 and SENP2). (**c** and **d**), Immunofluorescent analysis of SUMO1 (**c**) and SENP1 (**d**). Scale bars, 25 μm. (**e**), mRNA levels of genes involved in SUMOylation modification. Values represent the means ± SEM ($n = 3$ replicate tanks, and 6 fish were sampled from each tank). Significant variations at $P < 0.05$ are denoted by the letter (a-c)

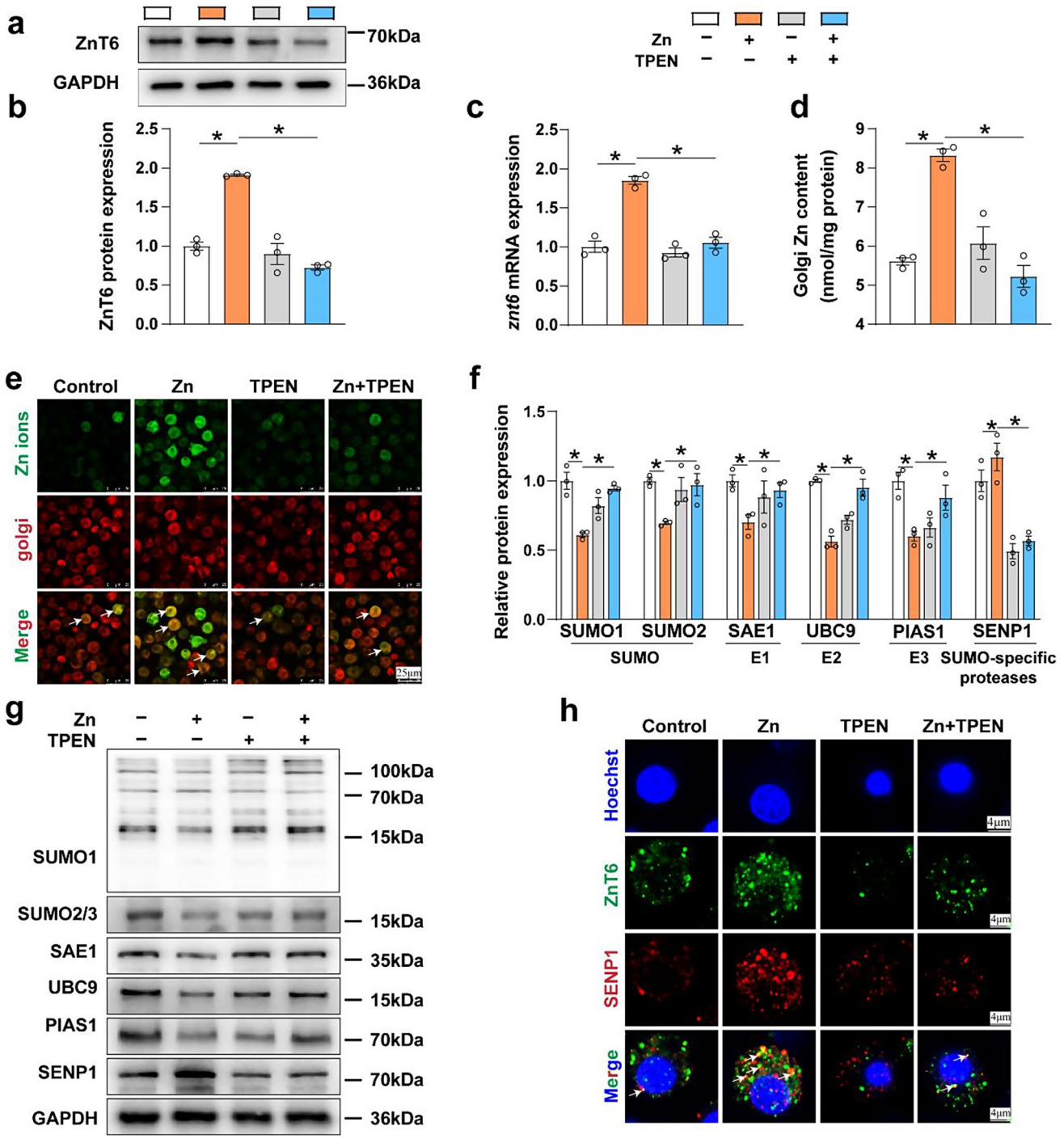

Fig. 3 TPEN attenuated Zn-induced increase in ZnT6 expression, decrease of SUMO level and the colocalization of ZnT6 and SENP1 in the hepatocytes of yellow catfish. (**a** and **b**), Western blot (**a**) and statistical analysis (**b**) of ZnT6. (**c**), mRNA level of *znt6*. (**d**), Zn content in Golgi apparatus. (**e**), Confocal microscopic image of Zn ions (green) co-localized with Golgi (red) by immunofluorescence staining. Scale bars, 25 μm. (**f** and **g**), Western blot and statistical analysis of the protein involved in pro-SUMOylation (SUMO1, SUMO2/3, SAE1, UBC9 and PIAS1) and de-SUMOylation (SENP1). (**h**), Confocal microscopy image of ZnT6 co-localized with SENP1 in yellow catfish hepatocytes detected by immunofluorescence staining using anti-ZnT6 (green) and anti- SENP1 antibodies (red). Scale bars, 4 μm. Values represent the means ± SEM ($n = 3$ independently biological experiments). The statistical significance (P value) was determined by Student's t test. *$P < 0.05$

vitro studies to determine whether MTF-1 mediates Zn-induced increase of *senp1* expression. TPEN pretreatment significantly alleviated Zn-induced increase of *mtf-1* mRNA expression (Fig. S2), total-MTF-1 and nuclear MTF-1 protein levels (Fig. 4a-b) in yellow catfish hepatocytes. Immunofluorescence analysis further confirmed these results (Fig. 4c-d).

Next, we performed promoter analysis of *senp1* gene to explore whether Zn-induced changes in Zn transporters expression was mediated by MTF-1 targeting the *senp1* gene. By analyzing the *senp1* promoter (Fig. S3), we predicted an evolutionary conserved MTF-1 binding sequence (MRE), which was located at −589 to −602 bp on yellow catfish *senp1* promoter (Fig. 4e). Furthermore, Zn treatment increased the luciferase activity of the *senp1* promoter (Fig. 4f), and these changes induced by Zn were alleviated by the MRE mutation on *senp1*, demonstrating that Zn triggered the activation of MTF-1, which in turn transcriptionally activated *senp1* via binding of MTF-1 to the MRE motif of the *senp1* promoter (Fig. 4f). Meanwhile, EMSA indicated that the putative MRE sequence of the *senp1* promoter could bind to nuclear extract, and the interaction could be disrupted by unlabeled probes but not by mutant probes (Fig. 4g and h). In addition, the binding activity of MTF-1 to MRE was significantly enhanced upon Zn incubation (Fig. 4g and h, lane 5), indicating that the −589 to −602 bp region of the *senp1* promoter was the functional site for its transcriptional regulation.

Then, small interference RNA si-*mtf1* was used to determine the correlation between MTF-1 and SENP1 in yellow catfish hepatocytes. According to mRNA and western blotting analysis, siMTF-1-2 had the highest knockdown efficiency and was selected for our experiment (Fig. S4A-C). The siMTF-1 pretreatment significantly alleviated the Zn-induced up-regulation of the SENP1 mRNA and protein levels (Fig. S4D-F). Overall, the above results demonstrated that the MRE mediated the transcriptional activation of *senp1* to Zn overload.

SENP1 mediated Zn-induced upregulation of the mRNA and protein levels of ZnT6

Having obtained strong evidence that Zn overload promoted SUMO-specific proteases expression and affected the expression of ZnT6, we further investigated the potential causal relationship between them via the small interference RNA (siRNA) against SENP1 expression. siSENP1-1 had the highest knockdown efficiency based on the results of mRNA and western blotting analysis (Fig. 5a-c). Immunofluorescence staining further corroborated that siSENP1-1 had the highest interference efficiency (Fig. 5d). Therefore, siSENP1-1 was selected for subsequent experiments. The *senp1* knockdown suppressed the Zn-induced up-regulation of SENP1 protein abundance (Fig. 5e and f). Furthermore, si-SENP1 treatment attenuated the increase of ZnT6 protein abundance induced by Zn (Fig. 5e and g). Collectively, these data indicated that Zn-induced increase of ZnT6 expression was mediated by SENP1.

ZnT6 was SUMOylated by SUMO1 and deSUMOylated by SENP1

To identify whether ZnT6 could be SUMOylated in cells and which type of SUMO could be conjugated with ZnT6, we transiently transfected HA-ZnT6 with the different types of SUMO (Myc-tagged SUMO1/2/3) into HEK-293T cells. Then, immunoprecipitation (IP) was conducted to determined SUMOylation of ZnT6. Cell lysates were collected and immunoprecipitated with anti-HA antibody. Anti-HA immunoblotting results showed a specific shifted band of SUMOylated-ZnT6. According to the gray value of the SUMOylated-ZnT6 band, we found that ZnT6 was modified mainly by SUMO1 (Fig. 6a). To further confirm the role of SUMO1 in the SUMOylation of ZnT6, we constructed a mutant SUMO1 by deleting the diglycine residues form the thioester linkage. Our results showed that ZnT6 SUMOylation can be detected only when ZnT6 is co-transfected with wild-type SUMO1 in HEK-293T cells, while SUMO1 mutant cannot (Fig. 6b). Our further immunofluorescence analysis revealed the co-localization between ZnT6 and SUMO1 (Fig. 6c). Therefore, we mainly focused on SUMO1-mediated SUMOylation of ZnT6 in the following experiments. To further verify whether the only E2-conjugating enzyme (UBC9) participated in the SUMOylation of ZnT6, we transfected HA-ZnT6 alone or in combination with Myc-tagged SUMO1, His-UBC9 into HEK-293T cells. We found that UBC9 overexpression significantly enhanced the SUMOylation of ZnT6, indicating the important role of UBC9 in ZnT6 SUMOylation modification (Fig. 6d, lanes 4). Co-immunoprecipitation (Co-IP) analysis revealed that HA-ZnT6 interacted with His-UBC9, indicating their physical link in HEK-293T cells (Fig. 6e and f). These results supported that ZnT6 was directly conjugated by SUMO1 in human cells.

SUMOylation is a dynamic process which was reversed by SUMO-specific proteases (SENPs), collectively known as deSUMOylase [22]. According to the released genome sequence, seven SENPs have been identified in yellow catfish (SENP1, 2, 3, 5, 6, 7 and 8) [39]. To identify which SENP removed the SUMO1 modification, SUMO1 and each of the seven SENPs were co-transfected with HA-ZnT6 into HEK-293T cells, and then SUMOylation of ZnT6 was determined. The results showed that SENP1 reduced ZnT6 SUMOylation level, while other SENPs did

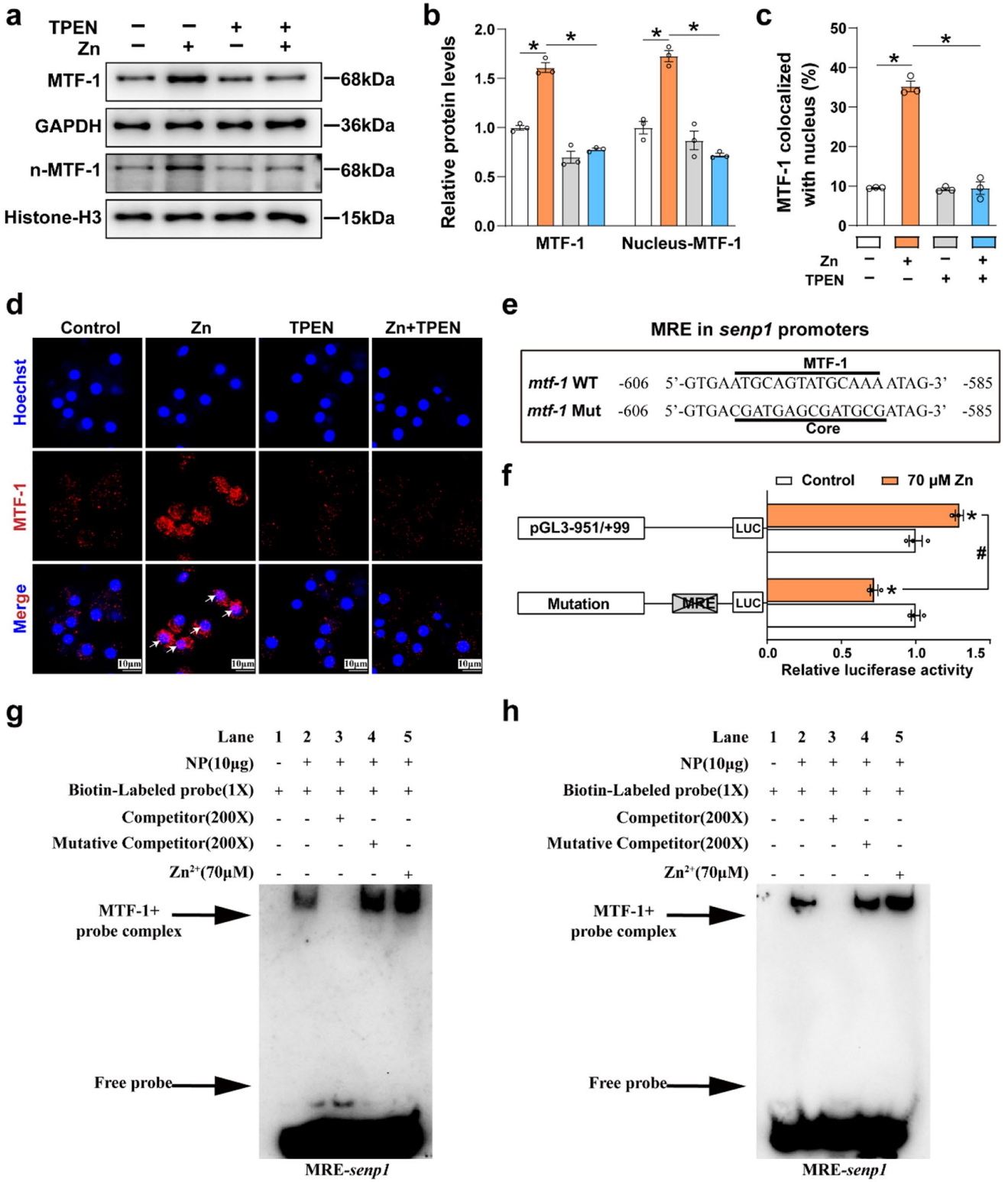

Fig. 4 Zn induced the upregulation of SENP1 expression by promoting the DNA binding of MTF-1 to the *senp1* promoter. (**a**-**b**), Western blot and statistical analysis of MTF-1 and n-MTF-1 (nucleus-MTF-1) in the hepatocytes of yellow catfish. (**c**-**d**), Immunofluorescent analysis of MTF-1 (**d**) and quantification of the co-localization between MTF-1 and nuclear (**c**). Scale bars, 10 μm. (**e**), MTF-1 binding sequence (MRE) located at − 589 bp to − 602 bp of *senp1* promoter of yellow catfish. (**f**), Site mutagenesis of MTF-1 on the pGl3- *senp1* -951/+99 vector. (**g** and **h**), EMSA analysis of predicted MTF-1 binding sequences (MRE) on the *senp1* promoter. The 5′-biotin labeled double-stranded oligomers were incubated with nuclear protein in HEK-293T cell (**g**) or yellow catfish hepatocytes (**h**). Values represent the means ± SEM ($n = 3$ independently biological experiments). Asterisk (*) and hash sign (#) represent significant differences at $P < 0.05$ between the two groups, as determined using Student's *t*-test

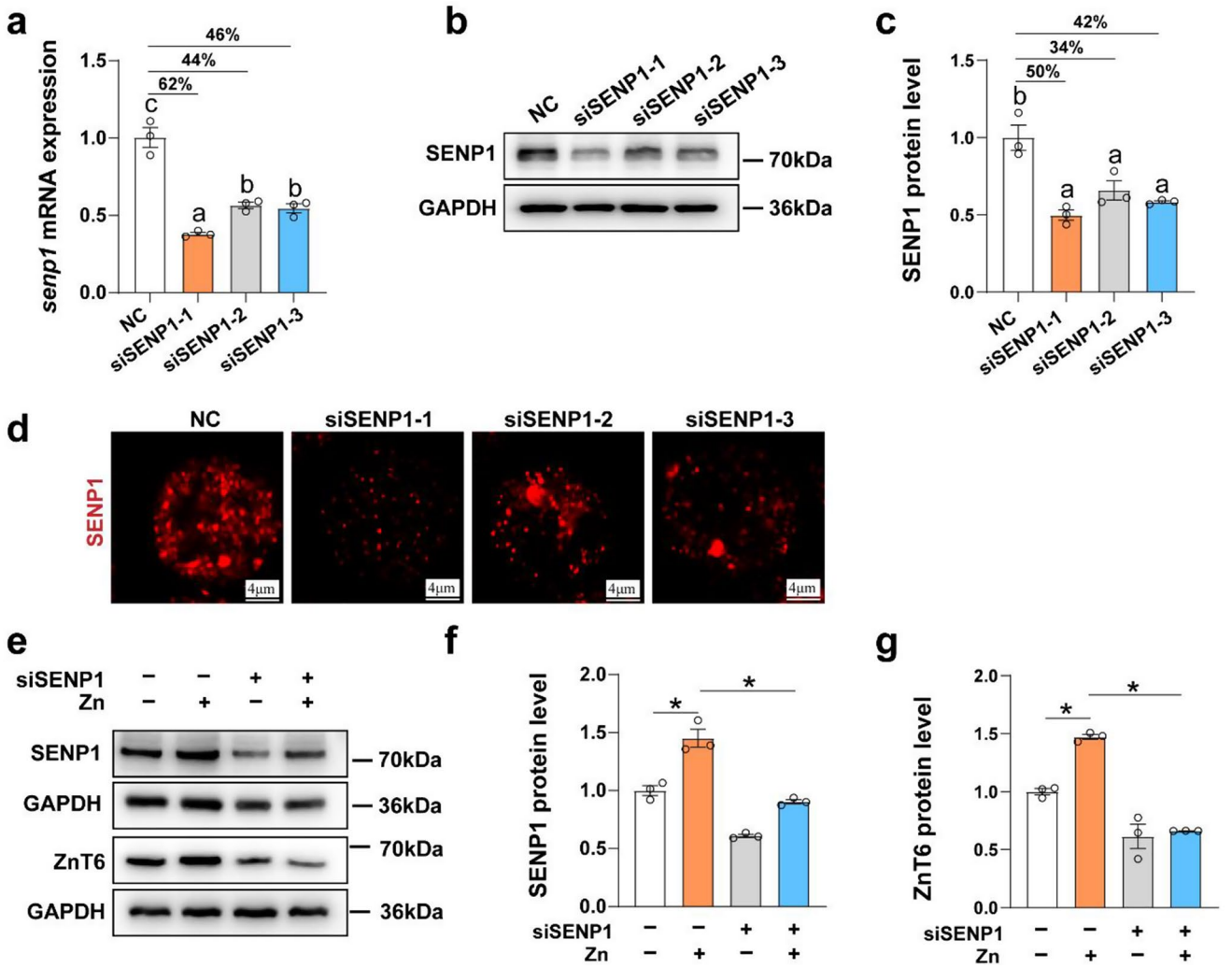

Fig. 5 The SENP1 mediated Zn-induced increase of ZnT6 expression in the hepatocytes of yellow catfish. (**a**-**c**), qPCR (**a**), Western blot and statistical analysis (**b** and **c**) of the knockdown efficiency of siRNA targeting *senp1* in hepatocytes. (**d**), Confocal microscopic image of the SENP1 protein detected by immunofluorescence staining. Scale bars, 4 μm. (**e**-**g**), Western blot and statistical analysis of SENP1 (**e** and **f**) and ZnT6 (**e** and **g**) protein expression. Values represent the means ± SEM ($n = 3$ independently biological experiments). The statistical significance (P value) was determined by Student's t test. $^*P < 0.05$

not influence ZnT6 SUMOylation level (Fig. 6g). In mammals, the C603A mutant of SENP1 did not have catalytic activity [41]. Importantly, sequence alignment found that C697 site of yellow catfish SENP1 (corresponding to C603 in mammalian SENP1) appears to be highly conservative among different species (Fig. S5). Thus, the overexpression vector of SENP1^{C697A} was generated from the full-length SENP1, which contains the mutant form of C697A (cystine was mutated to alanine at 697 position). We found that the wild-type SENP1 reduced the SUMOylation level of ZnT6, while the SENP1^{C697A} did not (Fig. 6h). The SUMOylation level of ZnT6 appeared to be decreased in a dose-dependent manner in the case of SENP1 overexpression (Fig. 6i), further confirming the critical role of SENP1 in mediating ZnT6 deSUMOylating. Furthermore, to determine whether Zn affected SUMOylation modification of ZnT6, HA-ZnT6, Myc-SUMO1 and His-UBC9 were co-transfected into HEK-293T cells and treated with or without indicated concentrations of Zn for 24 h, showing that Zn treatment greatly inhibited SUMOylation modification of ZnT6 (Fig. 6j). All above results proved that SENP1 was a crucial deSUMOylation enzyme for ZnT6 in human HEK-293T cells.

Lysine 409 (K409) was the major SUMOylation site of ZnT6

Based on the SUMOplot™ Analysis Program (http://www.abgent.com/sumoplot), the potential SUMOylation sites of ZnT6 were predicted, which were located on multiple lysine residues at amino acid positions K29, K47, K162 and K409 in yellow catfish. (Fig. 7a). To determine which of these

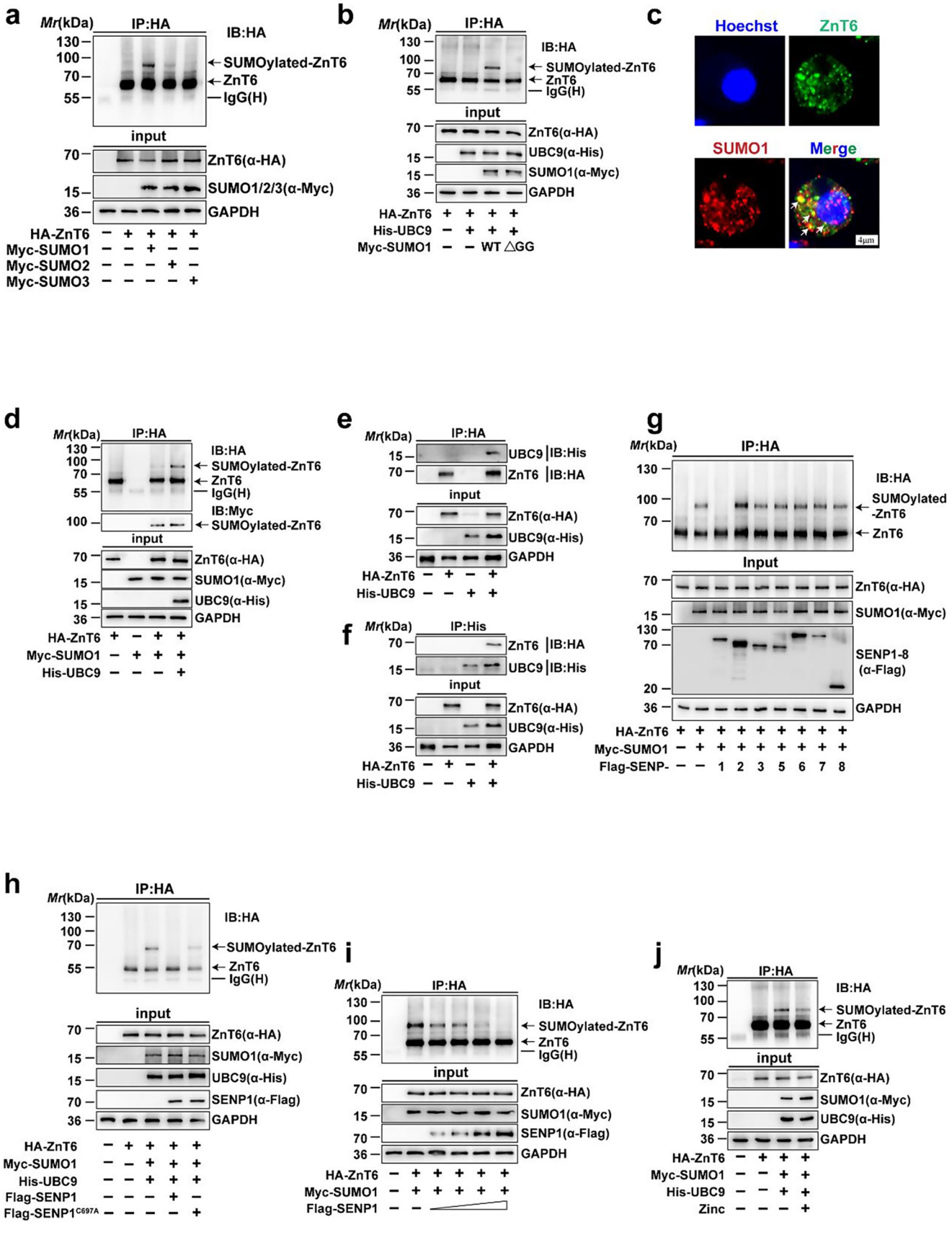
a
Mr(kDa)
IP:HA
IB:HA
130
100
70
55
SUMOylated-ZnT6
ZnT6
IgG(H)
input
70
ZnT6(α-HA)
15
SUMO1/2/3(α-Myc)
36
GAPDH
HA-ZnT6 − + + + +
Myc-SUMO1 − − + − −
Myc-SUMO2 − − − + −
Myc-SUMO3 − − − − +
b
Mr(kDa)
IP:HA
IB:HA
130
100
70
55
SUMOylated-ZnT6
ZnT6
IgG(H)
input
70
ZnT6(α-HA)
15
UBC9(α-His)
15
SUMO1(α-Myc)
36
GAPDH
HA-ZnT6 + + + +
His-UBC9 − + + +
Myc-SUMO1 − − WT △GG
c
Hoechst
ZnT6
SUMO1
Merge
4μm
d
Mr(kDa)
IP:HA
IB:HA
130
100
70
55
SUMOylated-ZnT6
ZnT6
IgG(H)
IB:Myc
100
SUMOylated-ZnT6
input
70
ZnT6(α-HA)
15
SUMO1(α-Myc)
15
UBC9(α-His)
36
GAPDH
HA-ZnT6 + − + +
Myc-SUMO1 − + + +
His-UBC9 − − − +
e
Mr(kDa)
IP:HA
15
UBC9 IB:His
70
ZnT6 IB:HA
input
70
ZnT6(α-HA)
15
UBC9(α-His)
36
GAPDH
HA-ZnT6 − + − +
His-UBC9 − − + +
f
Mr(kDa)
IP:His
70
ZnT6 IB:HA
15
UBC9 IB:His
input
70
ZnT6(α-HA)
15
UBC9(α-His)
36
GAPDH
HA-ZnT6 − + − +
His-UBC9 − − + +
g
Mr(kDa)
IP:HA
130
100
70
IB:HA
SUMOylated -ZnT6
ZnT6
Input
70
ZnT6(α-HA)
15
SUMO1(α-Myc)
130
70
20
SENP1-8 (α-Flag)
36
GAPDH
HA-ZnT6 + + + + + + + + +
Myc-SUMO1 − + + + + + + + +
Flag-SENP- − − 1 2 3 5 6 7 8
h
Mr(kDa)
IP:HA
130
100
70
55
IB:HA
SUMOylated-ZnT6
ZnT6
IgG(H)
input
70
ZnT6(α-HA)
15
SUMO1(α-Myc)
15
UBC9(α-His)
70
SENP1(α-Flag)
36
GAPDH
HA-ZnT6 − + + + +
Myc-SUMO1 − − + + +
His-UBC9 − − + + +
Flag-SENP1 − − − + −
Flag-SENP1C697A − − − − +
i
Mr(kDa)
IP:HA
130
100
70
55
IB:HA
SUMOylated-ZnT6
ZnT6
IgG(H)
input
70
ZnT6(α-HA)
15
SUMO1(α-Myc)
70
SENP1(α-Flag)
36
GAPDH
HA-ZnT6 − + + + + +
Myc-SUMO1 − + + + + +
Flag-SENP1 − −
j
Mr(kDa)
IP:HA
130
100
70
55
IB:HA
SUMOylated-ZnT6
ZnT6
IgG(H)
input
70
ZnT6(α-HA)
15
SUMO1(α-Myc)
15
UBC9(α-His)
36
GAPDH
HA-ZnT6 − + + +
Myc-SUMO1 − − + +
His-UBC9 − − + +
Zinc − − − +

Fig. 6 ZnT6 was mainly SUMOylated by SUMO1 and deSUMOylated by SENP1. (**a**), ZnT6 was mainly modified by SUMO1. HA-ZnT6 and Myc-SUMO1/2/3 were transfected into HEK-293T cells. The cell lysates were then IP with anti-HA antibody, followed by immunoblotting with the identical antibody. (**b**), Immunoprecipitation and immunoblot analysis of HEK-293T cells co-transfected with expressing vectors of HA-ZnT6, His-UBC9, Myc-SUMO1 and its indicated mutants. (**c**), Confocal microscopy image of ZnT6 co-localized with SUMO1 in yellow catfish hepatocytes detected by immunofluorescence staining using anti-ZnT6 (green) and anti-SUMO1 antibodies (red). Nuclear were stained blue. Scale bars, 4 μm. (**d**), UBC9 enhanced SUMOylation of ZnT6. HEK-293T cells were co-transfected with HA-ZnT6, Myc-SUMO1 and with or without His-UBC9, SUMOylated bands were then detected with anti-HA or anti-Myc antibody. (**e** and **f**), The interaction between ZnT6 and UBC9. The lysates of HEK-293T cells overexpression HA-ZnT6 and His-UBC9 were processed for IP with anti-HA (**e**) or anti-His (**f**) antibody, followed by immunoblot analysis with the reciprocal antibody. (**g**), SENP1, but not SENP2, 3, 5, 6, 7 and 8, deSUMOylated ZnT6. HA-ZnT6, Myc-SUMO1 and indicated isoforms of SENPs were transfected into HEK-293T cells, and then western blotting was performed to analyze the SUMOylation of ZnT6 with anti-HA antibody. (**h**), The deSUMOylated of ZnT6 is dependent on the catalytic activity of SENP1. HA-ZnT6, Myc-SUMO1 and His-UBC9 were transfected with wild-type SENP1 or the SENP1 C697A mutant into HEK-293T cells as indicated. Cell lysates were subjected to IP with anti-HA antibody, followed by immunoblot analysis using anti-HA antibody. (**i**), SENP1 down-regulated ZnT6 SUMOylation in a dose-dependent manner. HA-ZnT6 and Myc-SUMO1 were transfected into HEK-293T cells with varying amounts of Flag-SENP1, and then western blotting was performed to analyze the SUMOylation of ZnT6 using specified antibodies. (**j**), Zn incubation prevented ZnT6 from SUMOylation modification in HEK-293T cells. HA-ZnT6, Myc-SUMO1 and His-UBC9 were transfected into HEK-293T cells. After treatment with or without Zn (70 μM) for 24 h, the cell lysates were subjected to IP with anti-HA antibody, followed by immunoblotting with the same antibody to detect the SUMOylation of ZnT6 under Zn treatment. The band representing SUMOylation of ZnT6 was labeled with an arrow

lysine residues was the most important for SUMOylation of ZnT6 in yellow catfish, the Lys residues (K) were individually replaced with Arg residues (R). Then the plasmids expressing SUMO1 and UBC9 were co-transfected with WT or the mutant ZnT6 constructs into HEK-293T cells, and the levels of SUMOylation were analyzed as performed previously. Compared with wild-type ZnT6, mutants K29R, K47R and K162R did not cause significant changes in the SUMOylation levels of ZnT6 (Fig. 7b, lanes 4–6), and only the K409R mutant dramatically decreased ZnT6 SUMOylation level (Fig. 7b, lane 7), indicating that K409 of ZnT6 was the major SUMOylation site for SUMO1.

To further determine the role of lysine 409 in mediating ZnT6 SUMOylation modification. We replaced the two amino acid residues (phenylalanine and aspartic acid) on the flanking region of K409 with alanine to interrupt the consensus sequence of SUMOylation according to previous study [41]. Compared to the WT HA-ZnT6, HA-ZnT6-F408A/D410E co-expressed with Myc-SUMO1 significantly reduced SUMOylation levels of ZnT6, similar to HA-ZnT6-K409R (Fig. 7c). Importantly, sequence alignment revealed that K409 site of ZnT6 in yellow catfish is highly conserved in most of vertebrates (Fig. 7d). The protein structures of human ZnT6 were modeled in I-TASSER server (http://zhanglab.ccmb.med.umich.edu/I-TASSER/), and the structure of chitosan was downloaded from "PUB CHEM" database. The SUMOylation site of ZnT6 was picked up using the online tool pymol (https://sumo.biocuckoo.cn/) (Fig. 7e). Collectively, our results confirmed that K409 was the major site for SUMOylation modification of ZnT6 in yellow catfish.

ZnT6 SUMOylation did not affect its localization, but reduced its protein stability

SUMOylation participates in various signaling pathways and cellular processes by regulating the stability, subcellular location, transcriptional activity and interaction of targeted proteins [17–19]. To check whether SUMOylation modification affected the stability of ZnT6, the CHX assay was performed. HA-ZnT6-WT or HA-ZnT6-K409R was transfected into HEK-293T cells, followed by treatment with the protein translation inhibitor cycloheximide (CHX), for indicated time (0, 3, 6, 9 and 12 h). We found that the half-life of ZnT6-WT was shorter than that of the K409R mutation after CHX incubation (Fig. 8a). In addition, we also tested whether the stability of endogenous ZnT6 is affected by SUMOylation. SENP1 was knocked down by RNAi in yellow catfish hepatocytes. Knockdown of *senp1* remarkably decreased the half-life of endogenous ZnT6 (Fig. 8b). Taken together, our study confirmed that the protein stability of ZnT6 could be affected by the SUMO modification.

Next, we attempted to investigate whether the subcellular localization of ZnT6 was affected by SUMOylation. Immunofluorescence analysis confirmed that Zn incubation remarkably enhanced the protein expression of ZnT6 and its co-localization with the Golgi apparatus, while siSENP1 pretreatment alleviated this trend (Fig. 8c). At the same time, ZnT6 was mainly localized in the Golgi apparatus, and did not relocate under different levels of SUMOylation (Fig. 8c). In addition, compared with HA-ZnT6-WT, HA-ZnT6-K409R mutant did not significantly alter the subcellular localization of ZnT6 (Fig. 8d). Accordingly, our results demonstrated that ZnT6 SUMOylation did not alter its localization.

ZnT6 SUMOylation inhibited the increase of Zn content in Golgi apparatus induced by Zn

Our results above indicated that Zn reduced the SUMOylation level of ZnT6 by increasing the expression of SENP1. To further investigated the effect of ZnT6 SUMOylation level on Zn homeostasis in Golgi apparatus, SENP1 was knocked

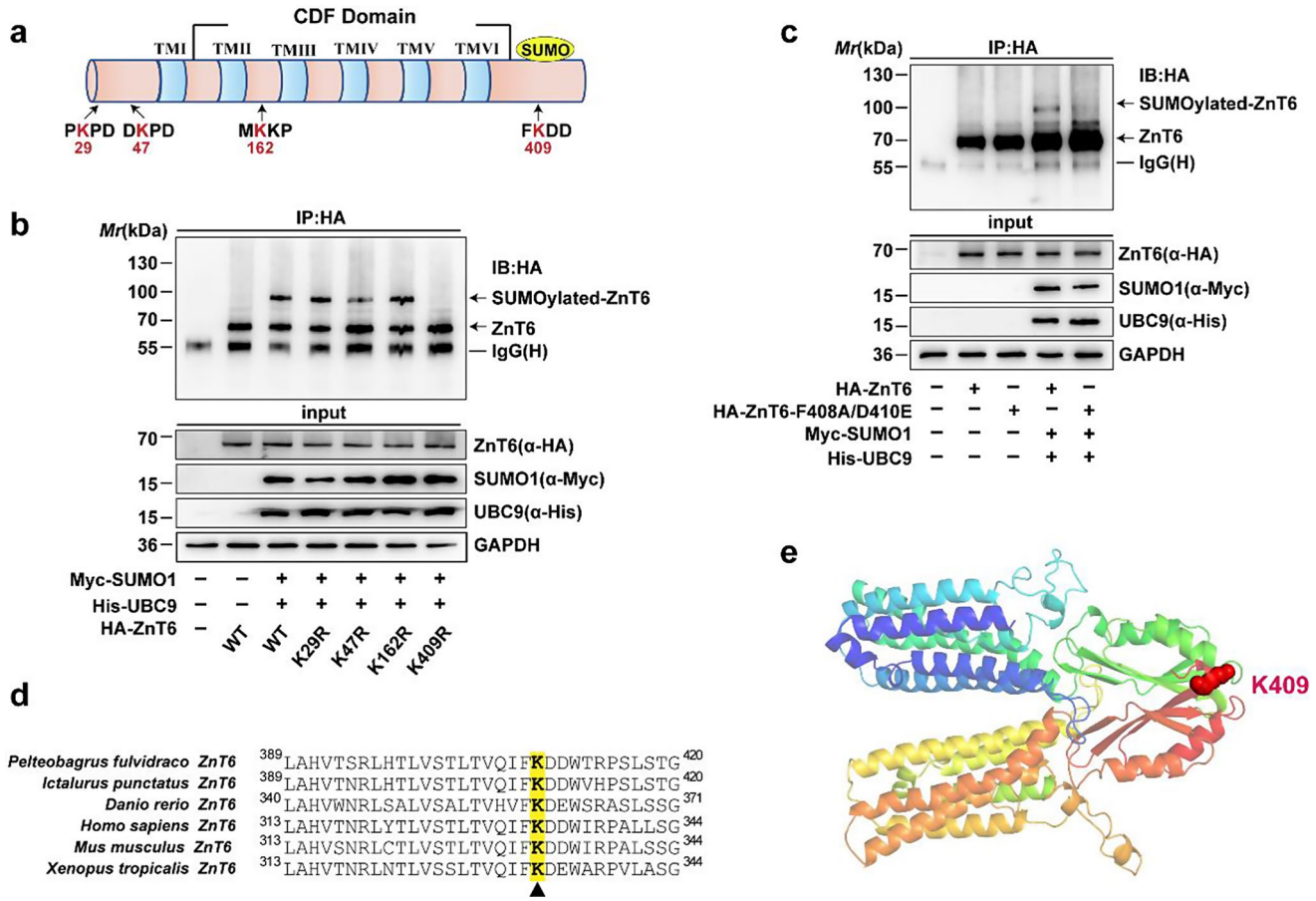

Fig. 7 Lysine 409 (K409) is the major SUMOylation site of ZnT6. (**a**), Prediction of four potential SUMOylation sites of ZnT6 in yellow catfish using SUMOplot software. (**b**), K409 was the major SUMOylation site in ZnT6. The lysates from HEK-293T cells overexpressing HA-ZnT6, HA-ZnT6 mutants (K29R/K47R/K162R/K409R), Myc-SUMO1 and His-UBC9 were IP with anti-HA antibody, and then immunoblot analysis was performed with the same antibody. (**c**), The mutant ZnT6-F408A/D410E further confirmed the SUMOylation of ZnT6. The lysates from HEK-293T cells overexpressing the indicated plasmids were IP with anti-HA antibody, and then immunoblot analysis was performed with the same antibody. (**d**), Sequences Alignment of ZnT6 from indicated species. The conserved lysine residue (K409) of SUMOylation modification is highlighted in yellow. (**e**), SUMOylation sites of yellow catfish ZnT6

down by RNAi in yellow catfish hepatocytes. Immunofluorescence analysis indicated that Zn treatment obviously increased the Zn content and its co-localization with the Golgi apparatus, while siSENP1 pretreatment alleviated this trend (Fig. 8e). In addition, the Zn content in Golgi apparatus was determined by ICP-OES. Knockdown of *senp1* remarkably alleviated Zn-induced increase of Zn content in Golgi apparatus (Fig. 8f). Taken together, SUMOylation of ZnT6 inhibited the increase of Zn content in Golgi apparatus induced by Zn.

Discussion

Despite the important role of SUMOylation modification in regulating biological processes, little is known about whether and how they affected Zn metabolism. Here, our present study demonstrated that ZnT6 was modified by SUMOylation and that hepatic Zn overload reduced ZnT6 SUMOylation making the protein more resistant to degradation and enabling sequestration of Zn in the Golgi apparatus. Mechanistically, MTF-1 stimulated transcription of *senp1*, inhibiting SUMO1-catalyzed ZnT6 SUMOylation modification via its K409 residue to help maintain Zn homeostasis in the Golgi apparatus. Overall, our findings for the first time reveal a novel mechanism for regulation of ZnT6 by SUMOylation modification.

The present study showed that liver Zn content increased with dietary Zn administration, consistent with previous studies [3]. Increasing evidence indicated that the imbalance of Zn homeostasis leads to various disease and is often attributable to the physiological dysfunction of different organelles [2, 10, 42]. The Golgi apparatus is an essential central membrane organelle, which play a pivotal role in protein processing and trafficking. Our investigation found that high dietary Zn supplementation increased the Zn content in

Golgi apparatus, indicating that the Golgi apparatus function as organelle storage for Zn, in agreement with other study [43]. Previous studies indicated that abnormal Zn^{2+} accumulation in the Golgi apparatus damaged the secretory pathway, leading to the occurrence of related diseases [10]. Therefore, it is very meaningful to study the subcellular distribution of Zn for maintaining Zn homeostasis and preventing pathological reactions related to the imbalance of Zn in Golgi apparatus.

Studies suggested that ZnT6 regulated uptake of Zn in Golgi apparatus [13]. In our study, high Zn levels promoted the upregulation of ZnT6 expression, indicating its involvement in the maintenance of Zn homeostasis by reducing cytosolic Zn. Similarly, previous studies demonstrated that Zn incubation upregulated the expression levels of both mRNA and protein for ZnT6 in yellow catfish hepatocytes [32]. Previous studies have revealed that ZnT5 recruit ZnT6 to form heterodimer complexes, which play an important role in biosynthetic by transferring zinc to the early secretory pathway, thereby activating enzymes that require zinc [7]. Our study indicated that high zinc up-regulated the protein expression level of ZnT5, in agreement with other studies [44]. As a Zn transporter located in the Golgi apparatus [13], the increased expression of ZnT6 promoted the transfer of cytosolic Zn to the Golgi, which was confirmed by the increasing Zn content in the Golgi apparatus by high dietary Zn. Similarly, previous study found that the increased ZnT6 led to the accumulation of Zn in trans-Golgi network (TGN) of degenerating neurons [45], indicating ZnT6 were involved in delivering Zn^{2+} into the TGN. The accumulation of Zn in the Golgi apparatus not only functioned as an indispensable cofactor for many secretory enzymes, but also alleviated the damage caused by excessive Zn in the cytosol. However, once the accumulation of Zn exceeds its normal range in Golgi apparatus, it will damage its physiological function of the Golgi apparatus and lead to the occurrence of related diseases. Therefore, these results collectively highlight a protective mechanism to maintain Zn homeostasis by regulating ZnT6-mediated Zn transport into the Golgi apparatus.

Although the impact of Zn on the post-translational modification of target proteins had been recognized, studies on the link between SUMOylation modification and Zn status remained largely unexplored [3, 46]. SUMOylation was mediated by SUMO protein and catalyzed by several specific enzymes, including activating enzyme E1, conjugating enzyme E2, and ligating enzyme E3 [17]. A previous study found that expression of SUMO1-modified proteins was decreased in Zn-deficient neonatal mice [47]. However, our study revealed that Zn reduced the expression of SUMO-proteins, SAE1/UBA2, UBC9 and PIAS1, was related to inhibition of SUMOylation modification induced by Zn. It has been reported that the SENP family can reverse the SUMOylation process [48]. Moreover, we found that Zn upregulated the expression of SENP1, SENP2 and SENP6, further confirming that Zn contributed to the deSUMOylation process of target proteins. In contrast, previous study confirmed that Zn decreased the expression of deSUMOylation enzymes (SENP2, SENP5 and SENP7), and increased the SUMOylation levels of target proteins [40]. This discrepancy might arise from distinct species-specific responses to Zn-induced SUMOylation modification. Overall, these data suggested that Zn-induced upregulation of SENP1 expression potentially facilitated SUMO1 deconjugation, thereby maintaining the balance between SUMOylation and deSUMOylation.

Studies suggested that Zn played a pivotal role in modulating SUMOylation at the cellular level [23]. However, the underlying regulatory mechanism remains unclear. Our study indicated that excessive dietary Zn enhanced both total and nuclear MTF-1 levels, and promoted nuclear translocation of MTF-1, consistent with previous reports [9]. By analyzing the structure of *senp* promoter in yellow catfish, we identified a functional MRE site of *senp1* promoter. The dual-luciferase reporter assays and EMSA indicated the significant role of Zn in facilitating MTF-1 translocation to the nucleus, where it bound to the MRE of *senp1* promoter and increased its expression. Notably, our research established the direct link between MTF-1 and SENP1, suggesting that MTF-1 was required for Zn-induced modulation of SUMOylation levels via regulating SENP1-driven deSUMOylation process.

SENP deSUMOylase family can reverse SUMOylation by catalyzing the removal of SUMO from the substrate proteins. Among SUMO-specific proteases, SENP1 acted as a deSUMOylase specifically targeting SUMO1-conjugates to regulate the function of substrates. Here, we found that knockdown of *senp1* alleviated the increase of ZnT6 expression induced by Zn, suggesting that ZnT6 was modified by SUMOylation. ZnT6 was localized in the Golgi apparatus and TGN, primarily responsible for the transfer of Zn from cytosolic into the Golgi apparatus and accordingly reducing cytosolic Zn content [13]. Based on SUMOylation analysis, we demonstrated that ZnT6 can be SUMOylated by all three SUMO protein (SUMO1, SUMO2 and SUMO3), but mainly by SUMO1. Similarly, in mammalian cells, certain substrates can undergo SUMOylation modification by all three SUMO1/2/3, whereas different substrates are specifically targeted by individual SUMO (SUMO1, SUMO2, or SUMO3) [49]. UBC9 could not only establish interactions with ZnT6 but also subsequently enhanced the SUMOylation level of ZnT6, consistent with other reports where UBC9 physically interacted with target proteins to increase its SUMOylation [18, 50]. Meantime, we found

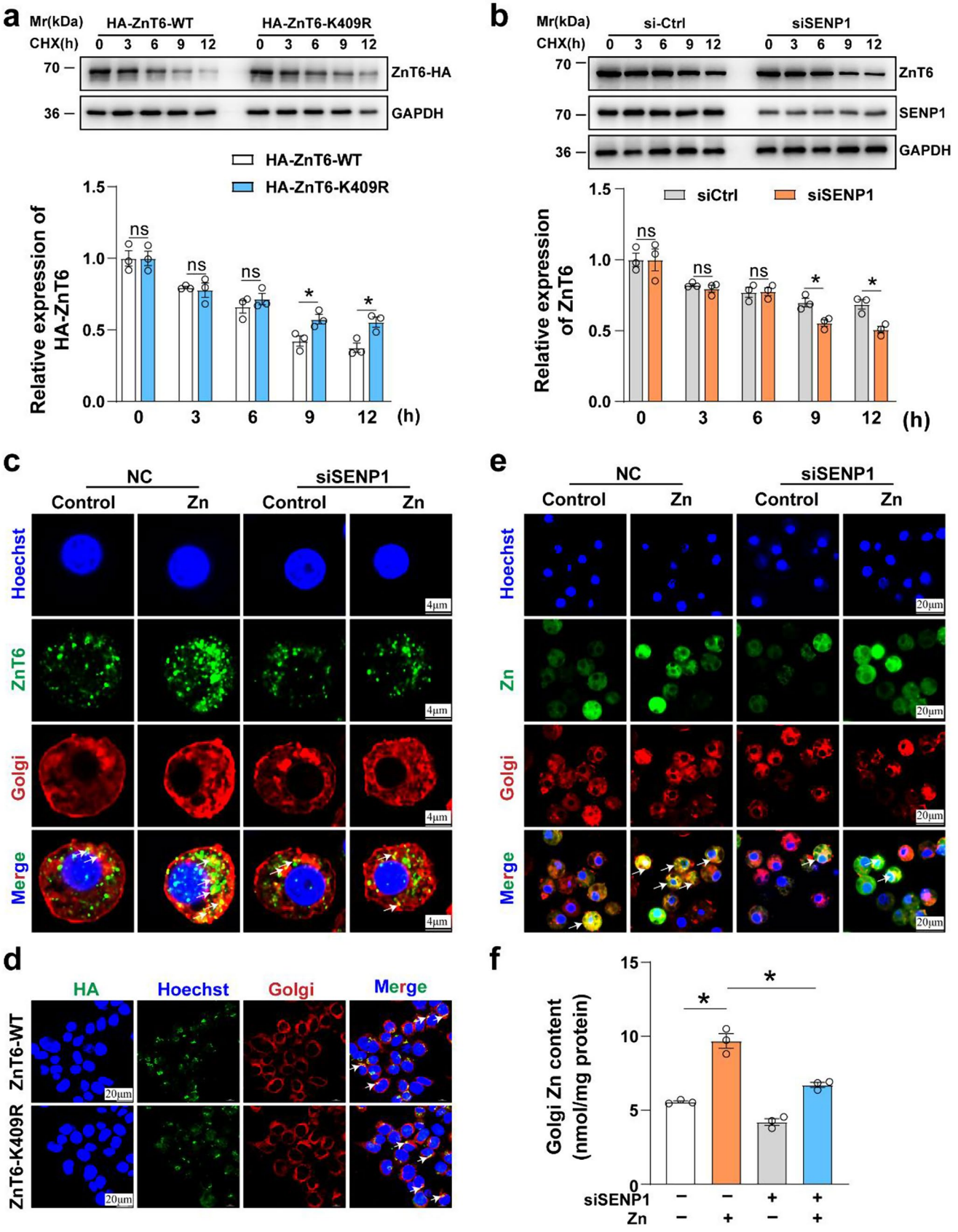
a
Mr(kDa)
HA-ZnT6-WT
HA-ZnT6-K409R
CHX(h) 0 3 6 9 12 0 3 6 9 12
70
ZnT6-HA
36
GAPDH
HA-ZnT6-WT
HA-ZnT6-K409R
Relative expression of HA-ZnT6
ns
*
(h)
b
Mr(kDa)
si-Ctrl
siSENP1
CHX(h) 0 3 6 9 12 0 3 6 9 12
ZnT6
SENP1
GAPDH
siCtrl
siSENP1
Relative expression of ZnT6
c
NC
siSENP1
Control
Zn
Hoechst
ZnT6
Golgi
Merge
4μm
e
20μm
d
HA
Hoechst
Golgi
Merge
ZnT6-WT
ZnT6-K409R
20μm
f
Golgi Zn content (nmol/mg protein)
siSENP1
Zn

Fig. 8 SUMOylation of ZnT6 did not affect its localization, but reduced its protein stability, inhibited the increase of Zn content in Golgi apparatus induced by Zn. (**a**), Western blotting analysis was performed to determine the half-life of ZnT6 by using anti-HA antibody in HEK-293T cells overexpressing wild-type ZnT6 or the ZnT6-K409R with or without CHX incubation for different time. (**b**), Western blotting analysis was performed to determine the half-life of endogenous ZnT6 by using anti-ZnT6 antibody in yellow catfish hepatocytes treatment with SENP1 knockdown with or without CHX incubation for different time. (**c** and **d**), ZnT6 SUMOylation did not change its subcellular localization. (**c**) Subcellular localizations of nuclear (blue), ZnT6 (green) with Golgi (red) were determined by confocal microscopy. Scale bars, 4 μm. (**d**) HEK-293T cells overexpressing wild-type ZnT6 or the ZnT6-K409R mutant were immunostained with ZnT6 (green), Golgi (red) and Hoechst (blue). Scale bars, 20 μm. (**e** and **f**), ZnT6 SUMOylation inhibited Zn-induced increases of the Zn content in Golgi apparatus. (**e**) Subcellular localizations of nuclear (blue), Zn ions (green) and Golgi (red) were determined by confocal microscopy. Scale bars, 20 μm. (**f**) Zn content in Golgi apparatus. Values represent the means ± SEM ($n = 3$ independently biolological experiments). The statistical significance (P value) was determined by Student's t test. $^*P < 0.05$

that SENP1 displayed deSUMOylating capabilities specific to ZnT6, as its ectopic expression diminished ZnT6 SUMOylation. Moreover, the mutation of the catalytic site of SENP1 (C697) increased the SUMOylation of ZnT6. Consistent with our result, other studies have shown that C603A inactivating mutation in mammal SENP1 upregulated the level of SUMOylation in target proteins, such as ZFHX3 [50] and PKCε [41]. Furthermore, since only one SUMOylation band was detected, we speculated that the SUMOylation site of ZnT6 might be restricted to a particular lysine residue. To identify this site, we individually replaced all 4 Lys residues with Arg. Our finding demonstrated that K409 was the major acceptor site, as evidenced by the significant reduction in SUMO1-modified ZnT6 upon the K409R mutation, which further confirmed our previous research [31]. Importantly, our study found that Zn inhibited ZnT6 SUMOylation, indicating that this modification was connected to metal homeostasis. Similarly, previous report indicated that the metal binding could interfere with the covalent and non-covalent interaction between SUMO1 and target proteins in the case of imbalanced Zn homeostasis [51], resulting in its dysfunction. Thus, we suggested that SENP1 was a sensor for elevating Zn levels, and SENP1-induced ZnT6 deSUMOylation was an important step in the regulation of Zn homeostasis.

Previous studies have confirmed that SUMOylation modulates the stability and subcellular localization of target proteins, influenced enzymes activity by altering the interactions among SUMOylated proteins [16–18]. Our current study showed that the ZnT6-K409R mutant was more stable than ZnT6-WT upon CHX treatment, suggesting that the stability of ZnT6 was attenuated by SUMOylation modification. Furthermore, siSENP1 reduced the stability of ZnT6, indicating that deSUMOylation protected ZnT6 from degradation. These results further explained that siSENP1 reduced the protein expression of ZnT6 mainly by reducing its protein stability and leading to protein degradation. Similarly, previous research indicated that protein stability could be inhibited by SUMOylation modification [20]. The disruption of SUMOylation can trigger the translocation of target protein from nucleus to the cytosol [50]. Nevertheless, studies have revealed that the target proteins modified by SUMOylation not only exist in the nucleus, but also distributed in various cellular components, such as mitochondria, endoplasmic reticulum, cytosol and the plasma membrane [52]. In our experiments, fluorescence imaging immunostaining assays demonstrated that neither the ZnT6-K409R mutant nor the knockdown of SENP1 had any impact on the localization of ZnT6, implying that SUMOylation of ZnT6 did not alter its subcellular localization, again similar to several other studies [29, 50, 53]. We also found that the Zn content in the Golgi apparatus decreased with the increase of the SUMOylation level of ZnT6 induced by siSENP1, indicating that the deSUMOylation of ZnT6 promoted the Zn transport from the cytosol into the Golgi apparatus to resist Zn overload and maintain intracellular Zn homeostasis. Accumulating evidence suggests that the disruption of zinc homeostasis is involved in various diseases, including cancer, cardiovascular disease, infectious immunity and neurodegenerative diseases [4, 5, 10, 54]. Furthermore, the Golgi zinc transporters have been identified to be associated with diseases [55, 56]. Among them, ZnT6 has been reported to be abnormally expressed in Alzheimer 's disease (AD) and Pick disease (PD), revealing the potential link between abnormal aggregation of Zn in the Golgi and pathogenesis [44, 57]. Given the impact of SUMOylation on the protein stability of ZnT6, we speculate that the regulation of SUMOylation modification of ZnT6 may be a potential target for disease treatment. Taken together, our study elucidated the roles of SUMOylation modification in Zn-induced change of ZnT6 expression, offering innovative insights for the understanding of the regulatory mechanisms and biological functions associated with ZnT6 in the future.

In summary, our results discovered a novel mechanism underlying SUMOylation modification of ZnT6 regulating the Zn homeostasis, as shown in Fig. 9. H-Zn regulated the absorption and transport of Zn, induced hepatic Zn accumulation and activated MTF-1/SENP1 pathway. We also demonstrated that SUMO1-catalyzed SUMOylation and SENP1-mediated deSUMOylation regulated ZnT6 activation, and K409 was the major SUMOylation site of ZnT6, and SUMOylation at K409 reduced the stability of ZnT6 but had no influence on localization of ZnT6. Thus, for the first time, we elucidated a novel mechanism by which SUMO1-catalyzed SUMOylation and SENP1-mediated

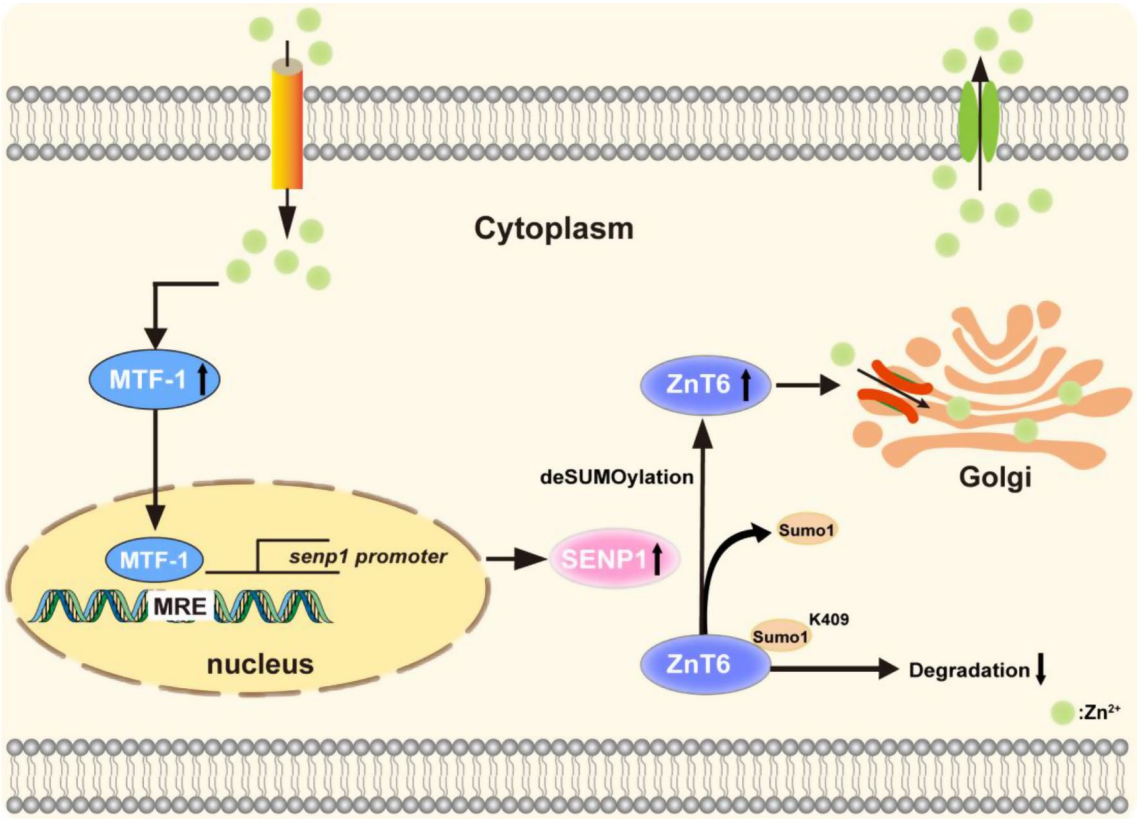

Fig. 9 A working model of MTF-1/SENP1 pathway-mediated ZnT6 deSUMOylation modification participating in the regulation of Zn metabolism in the Golgi apparatus

deSUMOylation of ZnT6 orchestrated the regulation of Zn metabolism within the Golgi apparatus.

Supplementary Information The online version contains supplementary material available at https://doi.org/10.1007/s00018-024-05452-4.

Acknowledgements The present study was funded by National Natural Science Foundation of China (32030111 and 31872585).

Author contributions The authors' responsibilities were as follows: C.C.S and Z.L. designed the experiments; C.C.S. conducted the experiments and sample analysis with the help of T.L., C.C.Z., and H.Z; C.H. and L.H.S. provided many critical suggestions for the experimental designs and data analysis; C.C.S. analyzed the data and drafted the manuscript; C.H. and Z.L. revised the manuscript; all authors read and approved the final manuscript.

Data availability The data that support the findings of this study are available from the corresponding author upon reasonable request.

Declarations

Ethical approval All experimental procedures were approved by the Ethics Committee of Huazhong Agricultural University (HZAU, Wuhan, China).

Consent to participate Not applicable.

Consent for publication All participants were properly consented.

Conflict of interest All the authors disclosed no conflict of interest.

References

1. Wei CC, Luo Z, Hogstrand C, Xu YH, Wu LX, Chen GH et al (2018) Zinc reduces hepatic lipid deposition and activates lipophagy via Zn^{2+}/MTF-1/PPARα and Ca^{2+}/CaMKKβ/AMPK pathways. FASEB J 32:6666–6680
2. Wu K, Luo Z, Hogstrand C, Chen GH, Wei CC, Li DD et al (2018) Zn stimulates the phospholipids biosynthesis via the pathways of oxidative and endoplasmic reticulum stress in the

intestine of freshwater teleost yellow catfish. Environ Sci Technol 52(16):9206–9214
3. Xu YC, Zheng H, Hogstrand C, Tan XY, Zhao T, Song YF et al (2023) Novel mechanism for zinc inducing hepatic lipolysis via the HDAC3-mediated deacetylation of β-catenin at lysine 311. J Nutr Biochem 121:109429
4. Ibs KH, Rink L (2003) Zinc-altered immune function. J Nutr 133:1452S–6S
5. Foster M, Samman S (2010) Zinc and redox signaling: perturbations associated with cardiovascular disease and diabetes mellitus. Antioxid Redox Signal 13(10):1549–1573
6. Sun W, Wang Y, Miao X, Wang Y, Zhang L, Xin Y et al (2014) Renal improvement by zinc in diabetic mice is associated with glucose metabolism signaling mediated by metallothionein and akt, but not Akt2. Free Radic Biol Med 68:22–34
7. Kambe T, Tsuji T, Hashimoto A, Itsumura N (2015) The physiological, biochemical, and molecular roles of zinc transporters in zinc homeostasis and metabolism. Physiol Rev 95(3):749–784
8. Kambe T, Hashimoto A, Fujimoto S (2014) Current understanding of ZIP and ZnT zinc transporters in human health and diseases. Cell Mol Life Sci 71(17):3281–3295
9. Chen GH, Lv WH, Xu YH, Wei XL, Xu YC, Luo Z (2020) Functional analysis of MTF-1 and MT promoters and their transcriptional response to zinc (zn) and copper (Cu) in yellow catfish *Pelteobagrus fulvidraco*. Chemosphere 246:125792
10. Li J, Wang Y (2022) Golgi metal ion homeostasis in human health and diseases. Cells 11(2):289
11. Gao J, Gao A, Zhou H, Chen L (2022) The role of metal ions in the golgi apparatus. Cell Biol Int 46(9):1309–1319
12. Amagai Y, Yamada M, Kowada T, Watanabe T, Du Y, Liu R et al (2023) Zinc homeostasis governed by Golgi-resident ZnT family members regulates ERp44-mediated proteostasis at the ER-Golgi interface. Nat Commun 14(1):2683
13. Huang L, Kirschke CP, Gitschier J (2002) Functional characterization of a novel mammalian zinc transporter, ZnT6. J Biol Chem 277(29):26389–26395
14. Fukunaka A, Suzuki T, Kurokawa Y, Yamazaki T, Fujiwara N, Ishihara K et al (2009) Demonstration and characterization of the heterodimerization of ZnT5 and ZnT6 in the early secretory pathway. J Biol Chem 284(45):30798–30806
15. Kambe T (2012) Molecular architecture and function of ZnT transporters. Curr Top Membr 69:199–220
16. Suzuki E, Ogawa N, Takeda TA, Nishito Y, Tanaka YK, Fujiwara T et al (2020) Detailed analyses of the crucial functions of zn transporter proteins in alkaline phosphatase activation. J Biol Chem 295(17):5669–5684
17. Li C, McManus FP, Plutoni C, Pascariu CM, Nelson T, Alberici Delsin LE et al (2020) Quantitative SUMO proteomics identifies PIAS1 substrates involved in cell migration and motility. Nat Commun 11(1):834
18. Hou G, Zhao X, Li L, Yang Q, Liu X, Huang C et al (2021) SUMOylation of YTHDF2 promotes mRNA degradation and cancer progression by increasing its binding affinity with m6A-modified mRNAs. Nucleic Acids Res 49(5):2859–2877
19. Jin S, He X, Ma L, Zhuang Z, Wang Y, Lin M et al (2022) Suppression of ACE2 SUMOylation protects against SARS-CoV-2 infection through TOLLIP-mediated selective autophagy. Nat Commun 13(1):5204
20. Wu X, Hu Y, Sui C, Pan L, Yoo D, Miller LC et al (2022) Multiple-site SUMOylation of FMDV 3 C protease and its negative role in viral replication. J Virol 96(17):e0061222
21. Seeler JS, Dejean A (2017) SUMO and the robustness of cancer. Nat Rev Cancer 17(3):184–197
22. Shao L, Liu Y, Wang W, Li A, Wan P, Liu W et al (2020) SUMO1 SUMOylates and SENP3 deSUMOylates NLRP3 to orchestrate the inflammasome activation. FASEB J 34(1):1497–1515
23. Liu YC, Lin MC, Chen HC, Tam MF, Lin LY (2011) The role of small ubiquitin-like modifier-interacting motif in the assembly and regulation of metal-responsive transcription factor 1. J Biol Chem 286(50):42818–42829
24. Thingholm TE, Rönnstrand L, Rosenberg PA (2020) Why and how to investigate the role of protein phosphorylation in ZIP and ZnT zinc transporter activity and regulation. Cell Mol Life Sci 77(16):3085–3102
25. Li M, Wang D (2017) Gene editing nuclease and its application in tilapia. Sci Bull 62(3):165–173
26. Minich JJ, Härer A, Vechinski J, Frable BW, Skelton ZR, Kunselman E et al (2022) Host biology, ecology and the environment influence microbial biomass and diversity in 101 marine fish species. Nat Commun 13(1):6978
27. Fang W, Chen Q, Cui K, Chen Q, Li X, Xu N et al (2021) Lipid overload impairs hepatic VLDL secretion via oxidative stress-mediated PKCδ-HNF4α-MTP pathway in large yellow croaker (*Larimichthys crocea*). Free Radic Biol Med 172:213–225
28. Luo Z, Tan XY, Zheng JL, Chen QL, Liu CX (2011) Quantitative dietary zinc requirement of juvenile yellow catfish *pelteobagrus fulvidraco*, and hepatic intermediary metabolism and antioxidant responses. Aquaculture 319:150–155
29. Ratn A, Prasad R, Awasthi Y, Kumar M, Misra A, Trivedi SP (2018) Zn^{2+} induced molecular responses associated with oxidative stress, DNA damage and histopathological lesions in liver and kidney of the fish, *Channa punctatus* (Bloch, 1793). Ecotoxicol Environ Saf 151:10–20
30. Zheng JL, Luo Z, Hu W, Liu CX, Chen QL, Zhu QL et al (2015) Different effects of dietary zn deficiency and excess on lipid metabolism in yellow catfish *pelteobagrus fulvidraco*. Aquaculture 435:10–17
31. Song CC, Wu LX, Chen GH, Chen GH, Lv WH, Chen SW et al (2020) Six members of SLC30A/ZnTs family related with the control of zinc homeostasis: characterization, mRNA expression and their responses to dietary ZnO nanoparticles in yellow catfish. Aquaculture 528:735570
32. Song CC, Chen GH, Zhong CC, Chen F, Chen SW, Luo Z (2021) Transcriptional responses of four slc30a/znt family members and their roles in Zn homeostatic modulation in yellow catfish *Pelteobagrus fulvidraco*. Biochim Biophys Acta Gene Regul Mech 1864(8):194723
33. Taylor KM, Hiscox S, Nicholson RI, Hogstrand C, Kille P (2012) Protein kinase CK2 triggers cytosolic zinc signaling pathways by phosphorylation of zinc channel ZIP7. Sci Signal 5(210):ra11
34. Song CC, Pantopoulos K, Chen GH, Zhong CC, Zhao T, Zhang DG et al (2022) Iron increases lipid deposition via oxidative stress-mediated mitochondrial dysfunction and the HIF1α-PPARγ pathway. Cell Mol Life Sci 79(7):394
35. Xu XW, Song CC, Tan XY, Zhong CC, Luo Z (2023) Effects of dietary zinc (zn) levels on growth performance, nutrient composition, muscle development, antioxidant and inflammatory responses in yellow catfish muscle. Aquaculture Rep 31:101640
36. Yang H, Du Y, Fei X, Huang S, Yimiti M, Yang X et al (2023) SUMOylation of the ubiquitin ligase component KEAP1 at K39 upregulates NRF2 and its target function in lung cancer cell proliferation. J Biol Chem 299(10):105215
37. Xu YC, Pantopoulos K, Zheng H, Zito E, Zhao T, Tan XY et al (2023) Phosphorus overload promotes hepatic lipolysis by suppressing GSK3β-dependent phosphorylation of PPARα at Ser84 and Thr265 in a freshwater teleost. Environ Sci Technol 57(6):2351–2361
38. Chen GH, Song CC, Pantopoulos K, Wei XL, Zheng H, Luo Z (2022) Mitochondrial oxidative stress mediated Fe-induced ferroptosis via the NRF2-ARE pathway. Free Radic Biol Med 180:95–107

39. Gong G, Dan C, Xiao S, Guo W, Huang P, Xiong Y et al (2018) Chromosomal-level assembly of yellow catfish genome using third-generation DNA sequencing and Hi-C analysis. GigaScience 7(11):giy120
40. Bian X, Xu J, Zhao H, Zheng Q, Xiao X, Ma X et al (2019) Zinc-induced SUMOylation of dynamin-related protein 1 protects the heart against ischemia-reperfusion injury. Oxid Med Cell Longev 2019: 1232146
41. Zhao X, Xia B, Cheng J, Zhu MX, Li Y (2020) PKCε SUMOylation is required for mediating the nociceptive signaling of inflammatory pain. Cell Rep 33(1):108191
42. Deng H, Qiao X, Xie T, Fu W, Li H, Zhao Y et al (2021) SLC-30A9 is required for Zn^{2+} homeostasis, Zn^{2+} mobilization, and mitochondrial health. Proc Natl Acad Sci USA 118(35):e2023909118
43. Lu Q, Haragopal H, Slepchenko KG, Stork C, Li YV (2016) Intracellular zinc distribution in mitochondria, ER and the golgi apparatus. Int J Physiol Pathophysiol Pharmacol 8(1):35–43
44. Liu LL, Song CC, Abu-Elala N, Tan XY, Zhao T, Zheng H et al (2024) Transcriptional regulation of Znt family members znt4, znt5 and znt10 and their function in zinc transport in yellow catfish (*Pelteobagrus fulvidraco*). Biochim Biophys Acta Gene Regul Mech 1867(3):195041
45. Lovell MA, Smith JL, Markesbery WR (2006) Elevated zinc transporter-6 in mild cognitive impairment, Alzheimer disease, and pick disease. J Neuropathol Exp Neurol 65(5):489–498
46. Wei X, Chen G, Xu Y, Zhang D, Lv W, Zheng H et al (2023) Zinc attenuates sulfamethoxazole-induced lipotoxicity by reversing sulfamethoxazole-induced mitochondrial dysfunction and lysosome impairment in a freshwater teleost. Chemosphere 345:140247
47. Zhang X, Wang C, Zhao D, Chen X, Zhang C, Zheng J et al (2020) Zinc deficiency induces abnormal development of the myocardium by promoting SENP5 overexpression. PLoS ONE 15(11):e0242606
48. Su Q, Chen X, Ling X, Li D, Ren X, Zhao Y et al (2023) SUMOylation of Smad2 mediates TGF-β-regulated endothelial-mesenchymal transition. J Biol Chem 299(10):105244
49. Ivanschitz L, Takahashi Y, Jollivet F, Ayrault O, Le Bras M, de Thé H (2015) PML IV/ARF interaction enhances p53 SUMO-1 conjugation, activation, and senescence. Proc Natl Acad Sci USA 112(46):14278–14283
50. Wu R, Fang J, Liu M, Liu AJ, Chen J W et al (2020) SUMOylation of the transcription factor ZFHX3 at Lys-2806 requires SAE1, UBC9, and PIAS2 and enhances its stability and function in cell proliferation. J Biol Chem 295(19):6741–6753
51. Kaur A, Jaiswal N, Raj R, Kumar B, Kapur S, Kumar D et al (2020) Characterization of Cu^{2+} and Zn^{2+} binding sites in SUMO1 and its impact on protein stability. Int J Biol Macromol 151:204–211
52. Huang J, Yan J, Zhang J, Zhu S, Wang Y, Shi T et al (2012) SUMO1 modification of PTEN regulates tumorigenesis by controlling its association with the plasma membrane. Nat Commun 3:911
53. Du Y, Hou G, Zhang H, Dou J, He J, Guo Y et al (2018) SUMOylation of the m6A-RNA methyltransferase METTL3 modulates its function. Nucleic Acids Res 46(10):5195–5208
54. Bafaro E, Liu Y, Xu Y, Dempski RE (2017) The emerging role of zinc transporters in cellular homeostasis and cancer. Signal Transduct Target Ther 2:17029
55. Giunta C, Elçioglu NH, Albrecht B, Eich G, Chambaz C, Janecke AR et al (2008) Spondylocheiro dysplastic form of the Ehlers-Danlos syndrome–an autosomal-recessive entity caused by mutations in the zinc transporter gene SLC39A13. Am J Hum Genet 82(6):1290–1305
56. Anzilotti C, Swan DJ, Boisson B, Deobagkar-Lele M, Oliveira C, Chabosseau P et al (2019) An essential role for the Zn^{2+} transporter ZIP7 in B cell development. Nat Immunol 20(3):350–361
57. Lyubartseva G, Smith JL, Markesbery WR, Lovell MA (2010) Alterations of zinc transporter proteins ZnT-1, ZnT-4 and ZnT-6 in preclinical Alzheimer's disease brain. Brain Pathol 20(2):343–350